AD-A040 709 RAYTHEON CO WALTHAM MASS RESEARCH DIV F/G 9/5
MANUFACTURING METHODS AND TECHNOLOGY MEASURE FOR ARC-PLASMA-SPR--ETC(U)
APR 77 H J VAN HOOK, R MAHER DAAB07-75-C-0043
UNCLASSIFIED S-2193 NL

1 OF 1
AD A040709

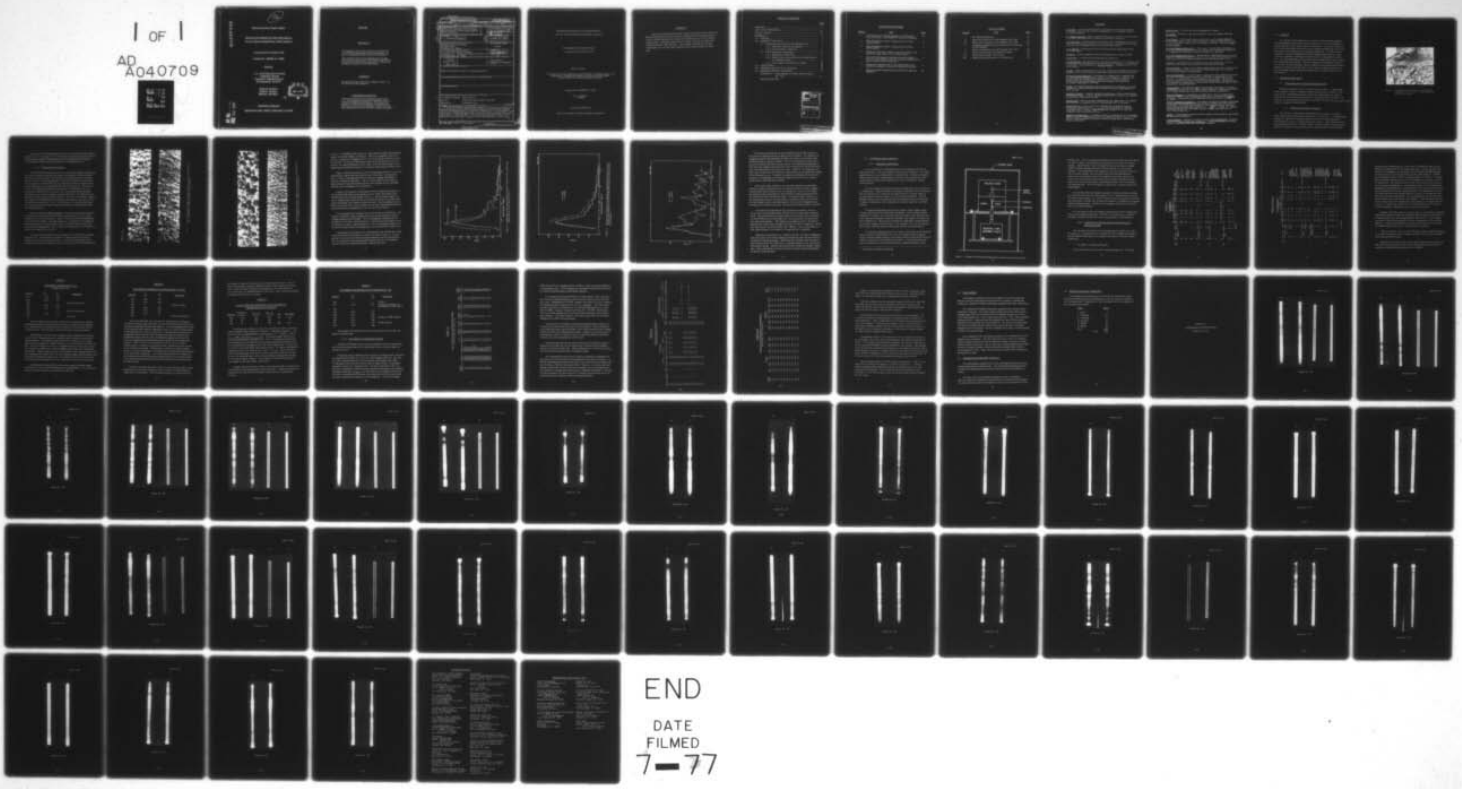

END

DATE FILMED
7-77

12

Seventh Quarterly Progress Report

Manufacturing Methods and Technology Measure For Arc-Plasma-Sprayed Phase-Shifter Elements

1 January 1977 to 31 March 1977

Contract No. DAAB07-75-C-0043

Placed by

U. S. Army Electronics Command
Production Division
Production Integrated Branch
Fort Monmouth, NJ 07703

Raytheon Company
Research Division
Waltham, MA 02154

Distribution Statement

Approved for public release; distribution unlimited

NOTICES

Disclaimers

The findings in this report are not to be considered as an official Department of the Army position, unless so designated by other authorized documents.

The citation of trade names and names of manufacturers in this report is not to be construed as official Government endorsement or approval of commercial products or services referenced herein.

Disposition

Destroy this report when it is no longer needed. Do not return it to the originator.

Acknowledgment Statement

"This project has been accomplished as part of the U.S. Army (Manufacturing and Technology) (Advance Production Engineering) Program, which has as its objective the timely establishment of manufacturing processes, techniques or equipment to insure the efficient production of current or future defense programs."

Unclassified

SECURITY CLASSIFICATION OF THIS PAGE (When Data Entered)

REPORT DOCUMENTATION PAGE

READ INSTRUCTIONS BEFORE COMPLETING FORM

1. REPORT NUMBER: Quarterly progress rept no. 7	2. GOVT ACCESSION NO.
3. RECIPIENT'S CATALOG NUMBER: 1 Jan - 31 Mar 77	
4. TITLE (and Subtitle): Manufacturing Methods and Technology Measure for Arc-Plasma-Sprayed Phase-Shifter Elements.	5. TYPE OF REPORT & PERIOD COVERED: Seventh Quarterly Progress 1 Jan. to 31 March 1977
	6. PERFORMING ORG. REPORT NUMBER: S-2193
7. AUTHOR(s): H. J. Van Hook, R. Maher	8. CONTRACT OR GRANT NUMBER(s): DAAB07-75-C-0043
9. PERFORMING ORGANIZATION NAME AND ADDRESS: Raytheon Research Division, 28 Seyon Street, Waltham, MA 02154	10. PROGRAM ELEMENT, PROJECT, TASK AREA & WORK UNIT NUMBERS: 2759441
11. CONTROLLING OFFICE NAME AND ADDRESS: U.S. Army Electronics Command, Production Div., Production Integration Branch, Fort Monmouth, NJ 07703	12. REPORT DATE: April 1977
	13. NUMBER OF PAGES: 68
14. MONITORING AGENCY NAME & ADDRESS (if different from Controlling Office): 71 p.	15. SECURITY CLASS. (of this report): Unclassified
	15a. DECLASSIFICATION/DOWNGRADING SCHEDULE

16. DISTRIBUTION STATEMENT (of this Report)

Approved for public release; distribution unlimited

17. DISTRIBUTION STATEMENT (of the abstract entered in Block 20, if different from Report)

18. SUPPLEMENTARY NOTES

19. KEY WORDS (Continue on reverse side if necessary and identify by block number)

Arc plasma spraying	Phase shifters
Ferrites	Microwave phase shifter materials
Dielectrics	Lithium ferrites

20. ABSTRACT (Continue on reverse side if necessary and identify by block number)

Twenty confirmatory samples and reports were delivered on January 30. Hysteresis loop and microwave testing at Raytheon and confirming measurements at ECOM Laboratories indicate the samples meet or exceed contract requirements. Differential phase shift on 10 test elements averages 384°, compared with the >340° specified. The average insertion loss on these 10 elements was 1.04 dB, which compares with a contract goal of 1 dB or less.

DD FORM 1 JAN 73 1473 EDITION OF 1 NOV 65 IS OBSOLETE

Unclassified

SECURITY CLASSIFICATION OF THIS PAGE (When Data Entered)

298320

Manufacturing Methods and Technology Measure For Arc-Plasma-Sprayed Phase-Shifter Elements

Seventh Quarterly Progress Report

1 January 1977 to 31 March 1977

Object of Study

"The objective of this manufacturing and methods technology measure is to establish the technology and capability to fabricate phase-shifter elements by the arc-plasma spraying techniques."

Contract No. DAAB07-75-C-0043

H. J. Van Hook
R. Maher

Distribution Statement

Approved for public release; distribution unlimited

ABSTRACT

Twenty confirmatory samples and reports were delivered on January 30. Hysteresis loop and microwave testing at Raytheon and confirming measurements at ECOM Laboratories indicate the samples meet or exceed contract requirements. Differential phase shift on 10 test elements averages 384°, compared with the >340° specified. The average insertion loss on these 10 elements was 1.04 dB, which compares with a contract goal of 1 dB or less.

TABLE OF CONTENTS

LIST OF ILLUSTRATIONS

LIST OF TABLES

GLOSSARY

Annealing - A heating schedule similar to firing but performed on a dense material to relieve strain, improve homogeneity or recrystallize a microcrystalline material.

Arc Plasma Spraying - High-temperature deposition technique in which molten or partially molten material is sprayed onto a heated substrate.

Coercive Force - The horizontal displacement of the magnetization vs applied field curve the hysteresis loop at zero induced field. A measure of the energy required to move magnetic domains through a solid material.

Core Material - The dielectric material which fills the hollow space within the ferrite toroid.

Dielectric - Oxide compounds which exibit polarization in electric fields.

Dilatometer - A device for measuring thermal expansion.

Elastic Modulus - The ratio of stress-to-strain (in pounds/in.^{2} or Newtons/in.^{2}) in isotropic materials which gives an indication of the stiffness or resistance to deformation. Also referred to as Young's modulus. Typically 10 to 50 $\times$ 10^6 psi for oxides.

Ferrite - Oxide compounds of iron and other elements that exhibit a spontaneous magnetic moment due to magnetic spin dipole alignment within the structure.

Hysteresis Loop Properties - The display of magnetization vs applied field for a toroidal or long rod-shaped sample of a ferromagnetic material. The display, generally obtained or low frequencies ($\leq$ 102 Hz) is useful in predictions of the magnetization properties and phase shift behavior at microwave frequencies ($\approx$ 10^{10} Hz).

Firing - Any high-temperature process performed on a material, but usually referring to a heating schedule which transforms a powder aggregate into a dense ceramic.

Isostatic Pressure - A powder compaction technique in which a sealed deformable container (e.g., a rubber bag with powder inside) is subject to a uniform compacting pressure from all sides.

Latched State - State of remnant magnetization after application of an applied field sufficient to magnetize in one or two opposite (180°) directions.

Lithium Ferrite - A class of ferrite materials with the general formula $Li_{.5+\,x/2\,-\,y2}\,Ti_xZn_{y2}\,Fe_{2.5\,-\,3x/2-y}O_4$ characterized by a saturation magnetization of $0 < 4\pi M_s < 3600$, a dielectric constant $18 < K < 20$, and frequently used in microwave devices.

Magnetic Compensation - A condition obtained in a specific ferrite composition and/or at specific temperatures where the magnetic moment is zero. At this point the opposed magnetic sublattices within the single phase composition exactly compensate.

Magnetometer - A device for measuring magnetic moment.

Microwave - That part of the electromagnetic spectrum between 100 MHz and 100 GHz.

Phase Shifter - A microwave device which serves as the active element in phased-array radar systems where the state of magnetic polarization is used to control the phase length of the electromagnetic energy. Also called phase control element.

Remanent Magnetization ($4\pi M_r$) - The value of induced field remaining in a material with toroidal geometry at zero applied field following the application of an applied field sufficient to uniformly magnetize a material.

Saturated Magnetization ($4\pi M_s$) - The saturation magnetization (c.g.s.) is the magnetic moment gauss/cm^3 of a material in an external DC field of sufficient magnitude to align the magnetic moment in the material parallel with it.

Saw Kerf - That portion of a solid removed by the cutting blade. The kerf width is usually about 5 percent wider than the width of the blade.

Spinel Ferrites - A class of iron oxide compositions having face-centered cubic crystal structures similar to the mineral spinel ($MgAl_2O_4$) and a magnetic moment which depends on composition.

Spray-Dried Powder - A form of powder aggregation where spherical particles of ~ 10 to 100 μm are produced which are themselves aggregates of much smaller (< 1 μm) particles. The advantage of this process is that the aggregates have better flow properties than untreated powder. The process is accomplished in a spray drier, a large funnel-shaped cavity into which a liquid suspension is sprayed and dried.

Stoichiometric - The idealized atomic proportions of elements in a chemical composition, such as the 1:2 in Mg:Al ratio in $MgAl_2O_4$. Departures from the exact integral proportions may have important effects on properties.

Stress-to-Failure - A statistical or average stress level of a solid where failure by brittle fracture propagation takes place, also called the modulus of rupture. Depends on surface conditions as well as intrinsic strength.

Thermal Expansion Coefficient - A parameter denoting the change in dimension ($\Delta l / l_o$) per unit temperature between ambient conditions and some elevated temperature. Since the actual expansion is not perfectly linear, one must specify the thermal interval of interest; i.e., $\alpha_{20°}^{1000°}$ = 15 ppm °C^{-1} denotes expansion between 20°C and 1000°C has our average slope $\Delta l / l_o \Delta T$ of $+15 \times 10^{-6}$ in./in./°C.

Toroid - A ring-shaped specimen used in magnetic measurements, particularly the hysteresis properties.

X-Ray Analysis - Analysis of crystal structure (X-ray diffraction), elemental composition (X-ray fluorescent analysis) to control processing or elucidate property variations using short wavelength radiation.

1.0 PURPOSE

The purpose of this program is to develop a manufacturing capability for producing the Patriot phase-shifter element by arc-plasma spraying of a lithium-titanium ferrite onto a dielectric substrate. The primary objective is to produce the phase control element as a finished composition with acceptable microwave properties and a reasonably high yield. To achieve sound composites, one of the properties needing constant monitoring is the match in thermal expansion coefficient between the ferrite coating and the dielectric. A second important area for control and reproducibility is the thermal environment during spraying. Thermal conditions are influenced mainly by arc current, the gas velocities, and the substrate-to-gun separation distance. Finally, to achieve a low unit cost, it is necessary to improve yield and reduce machining costs by working with local machine shops to improve overall efficiency.

2.0 NARRATIVE AND DATA

2.1 Preparation and Testing of Starting Materials

During this quarter we have continued to use the higher magnetization ferrite powder, which we designate LMTF475(G5) and LMTF475(G7). This is the ferrite composition primarily used in the confirmatory run, and we expect to use it in the pilot production run, which begins in early April. The dielectric composition has the nominal composition $Li_{1.0}Mn_{.10}Ti_{1.0}Al_{.07}Fe_{.83}O_4$, which we designate LMTAF200(7A).

2.1.1 Dielectric materials development

The dielectric composition LMTAF200(7A) is produced in 1-kg bars whose approximate external dimensions are $8 \times .85 \times 2.25$ in. A small amount of Bi_2O_3 (0.1 percent by weight) is added to lower the firing temperature. Fired density is 4.0 g/cc; typical grain size is 50 μm. The scanning electron photomicrograph in Fig. 1 at 1000× shows a fracture surface at the interface between the dielectric (large grains) and the annealed ferrite (small grains).

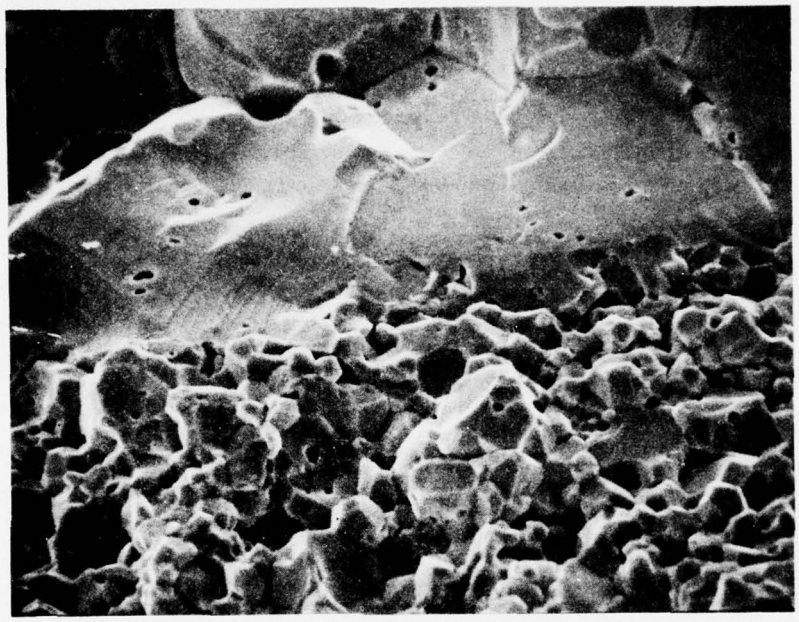

Figure 1 Scanning Electron Photomicrograph of the Boundary of the Dielectric, LMTAF200(7A), and Ferrite Powder.

As reported in the Fifth Quarterly Report, thermal expansion coefficient at 1000°C is $\bar{\alpha}$ = 15.2 ppm/°C. The slot geometry pictured in Fig. 16 of the Sixth Quarterly Report (long dimension of slot parallel to the surface between dielectric halves) has been adopted for the production run.

2.1.2 Ferrite powder evaluation

The LMTF475(G5) powder used in the confirmatory sample run had good flow characteristics and produced coatings with magnetic properties which satisfied our contract goals. We therefore wanted the powder for the pilot production run to have identical basic composition and flow characteristics. The new powder, LMTF475(G7), has been formulated from the same raw materials following the same processing and spray drying as G5. As far as we can tell, its magnetic and dielectric properties are identical to G5. Its powder flow characteristics, however, are very similar but not identical. Although the flow of the G5 powder was generally better, the differences are not large enough to create serious problems. We have, for example, sprayed APS samples with both powders and obtained comparable $4\pi M_r$ and H_c values, as will be discussed in Sec. 2.2.2. Nevertheless, we have decided to measure spray-dried particle size on these two powders to establish any differences quantitatively.

Figure 2 shows one SEM photograph of spray-dried G5 powder from the chambers fraction and one from the fines fraction collected in the cyclone separator at the exit end of dryer. Figure 3 shows similar SEM photographs of the G7 ferrite powder. The photographs are a collection of six sequential individual photos of a representative region of powder samples taken originally at 400× magnification. Size reduction for publication in this report has reduced the magnification to 175×.

The spray-dried particles in a photograph were counted at the original magnification. To determine the number of counts needed to generate a histogram representative of the sample, we divided the photograph in half and generated separate histograms of the two parts, approximately 800 counts

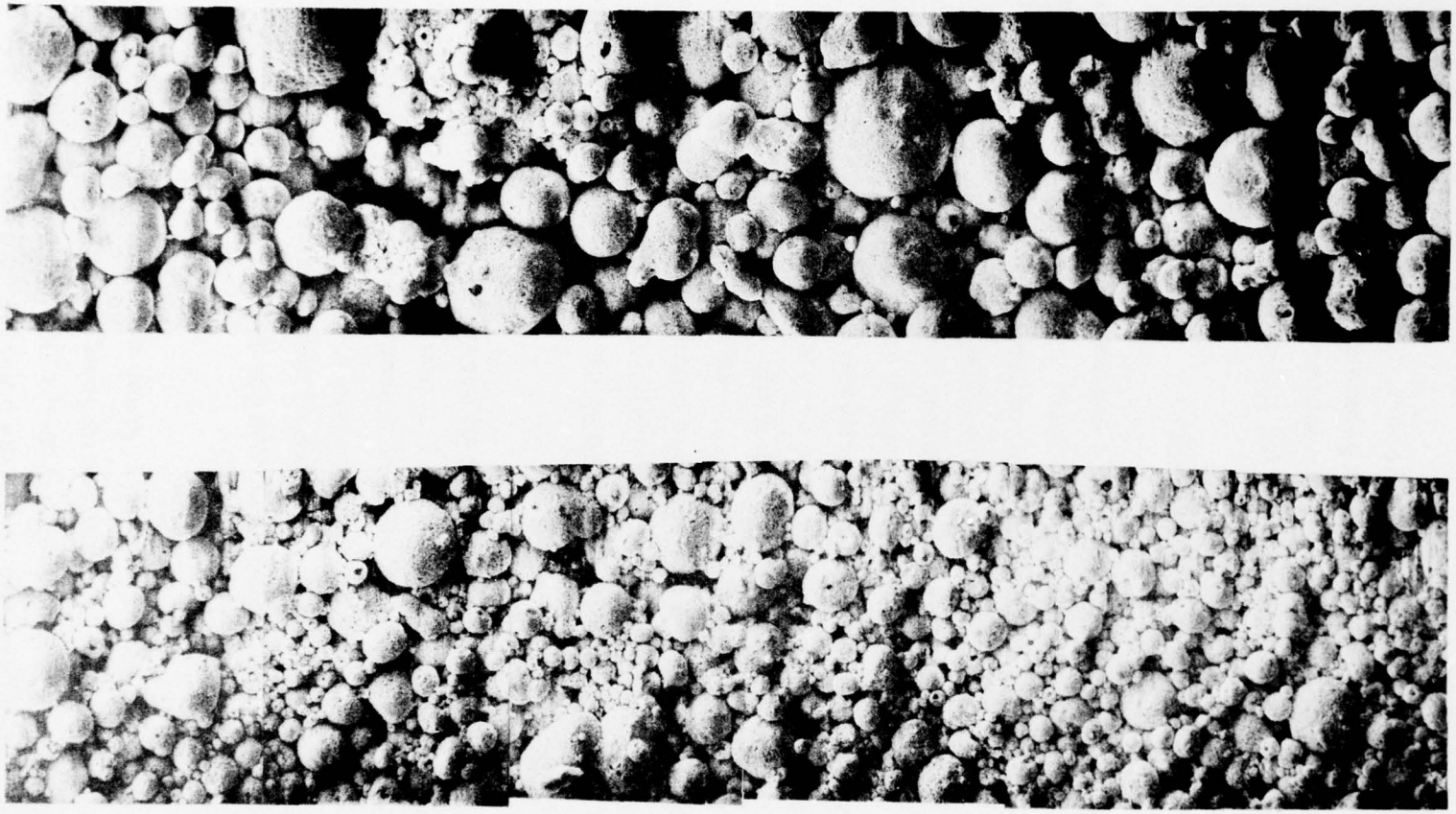

Figure 2 SEM Photographs at 400× of Spray-Dried Ferrites LMTF475(G-5).
Top: Chambers fraction; Bottom: Fines fraction.

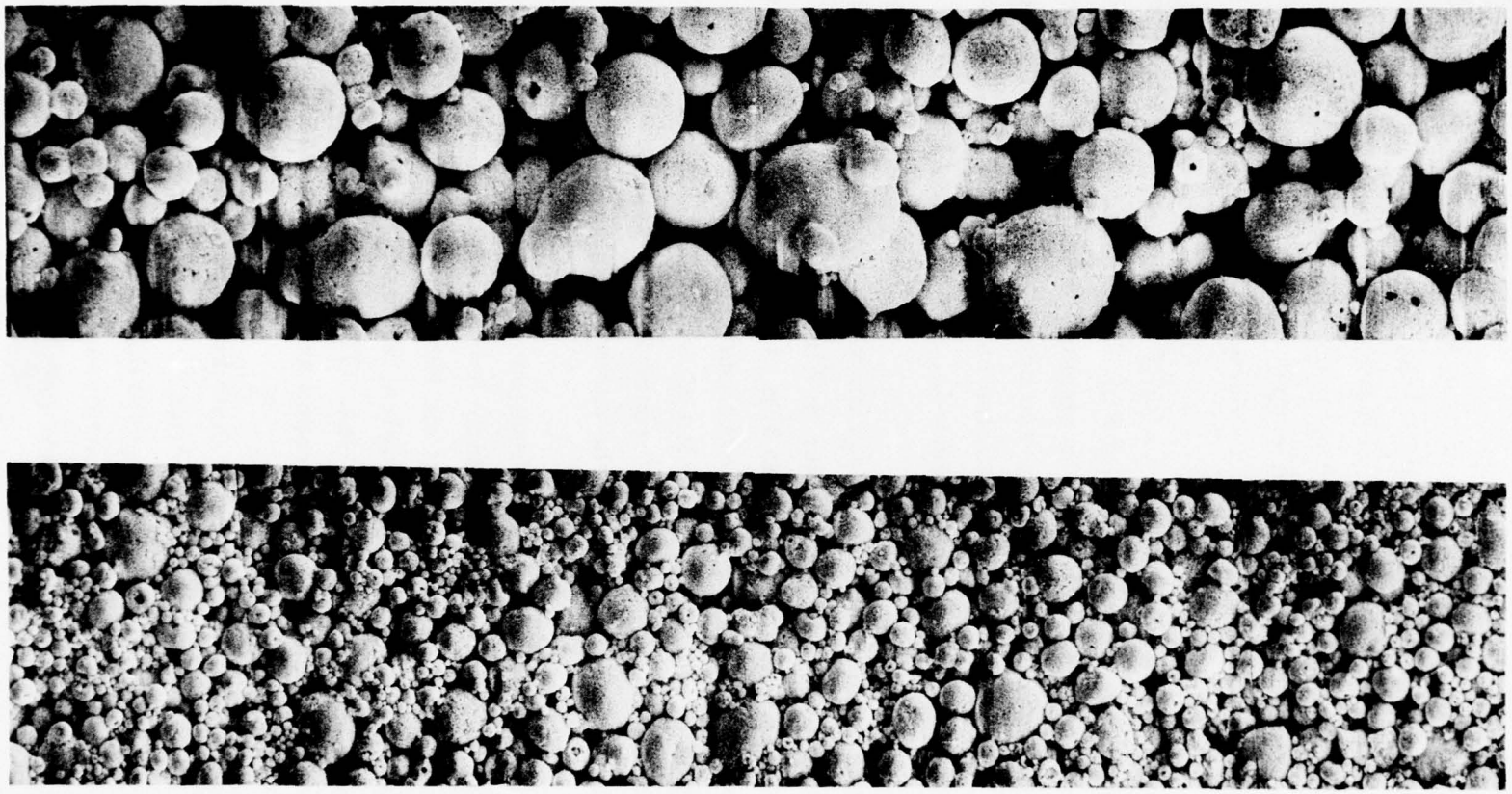

Figure 3 SEM Photographs at 400× of Spray-Dried Ferrites LMTF475(G-7).
Top: Chambers fraction; Bottom: Fines fraction.

in each. If a doubling of the number of counts does not change the histogram shape, the smaller number is adequate. What is an adequate count is, of course, a subjective evaluation, and we have had to adopt arbitrary criteria to set limits. We have decided that a change in mean particle size of > 20 percent, or radical differences in the shapes of the two distribution curves, would indicate insufficient data for a histogram representative of the powder.

Figure 4 shows two curves for the G7 fines powder fraction – one curve indicating the count in the lower half of Fig. 3; the other, the top half of Fig. 3. Every resolvable particle was counted, totalling 1672 different particles of different diameters. The two curves differ in mean value by approximately 15 percent and the particles have similar sizes, indicating that this count is adequate by our standards.

Figure 5 is a particle size histogram which compares 1454 counts of the LMTF475(G5) fines fraction powder in Fig. 2 with 1672 counts of the LMTF475(G7) fines fraction powder in Fig. 3. The G7 powder appears to have a slightly larger particle size at the peak area below 10 microns and a larger proportion of the larger particles as well. The histograms have not been corrected for the 13 percent difference in total counts between powders, which would alter the appearance of the curves to some degree.

We also studied the chambers fraction of the G5 and G7 powders. The number of particle counts is significantly less for these powders, and the counting statistics less reliable. The six photographs making up the G5 chambers view in Fig. 2 had 325 particles, whereas the total number for the G7 chambers in Fig. 3 was 261 particles. The corresponding numbers for the fines fraction in these two photographs are 1454 and 1672, respectively.

Histograms of the particle size distribution for the smaller size range of the G5 (0) and G7 (x) chambers fractions are shown in Fig. 6. A comparison of the two curves does not suggest differences in size distribution that seem apparent when comparing photographs; that is, the G7 powder seems to have more uniform and larger particles than G5.

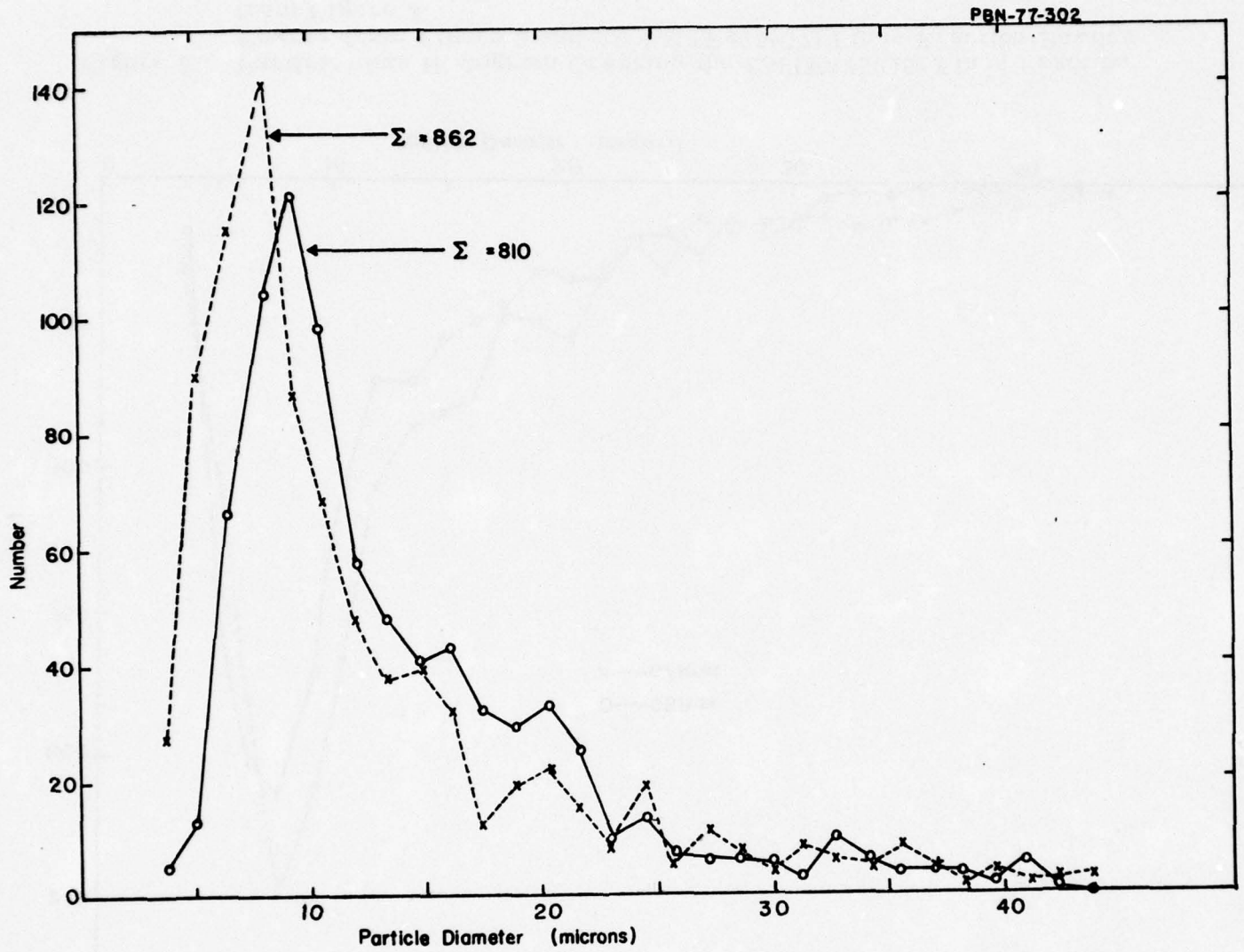

Figure 4 Histogram of G7 Fines Powder Fraction Counted on the Lower and Upper Halves of the Photo in Fig. 3.

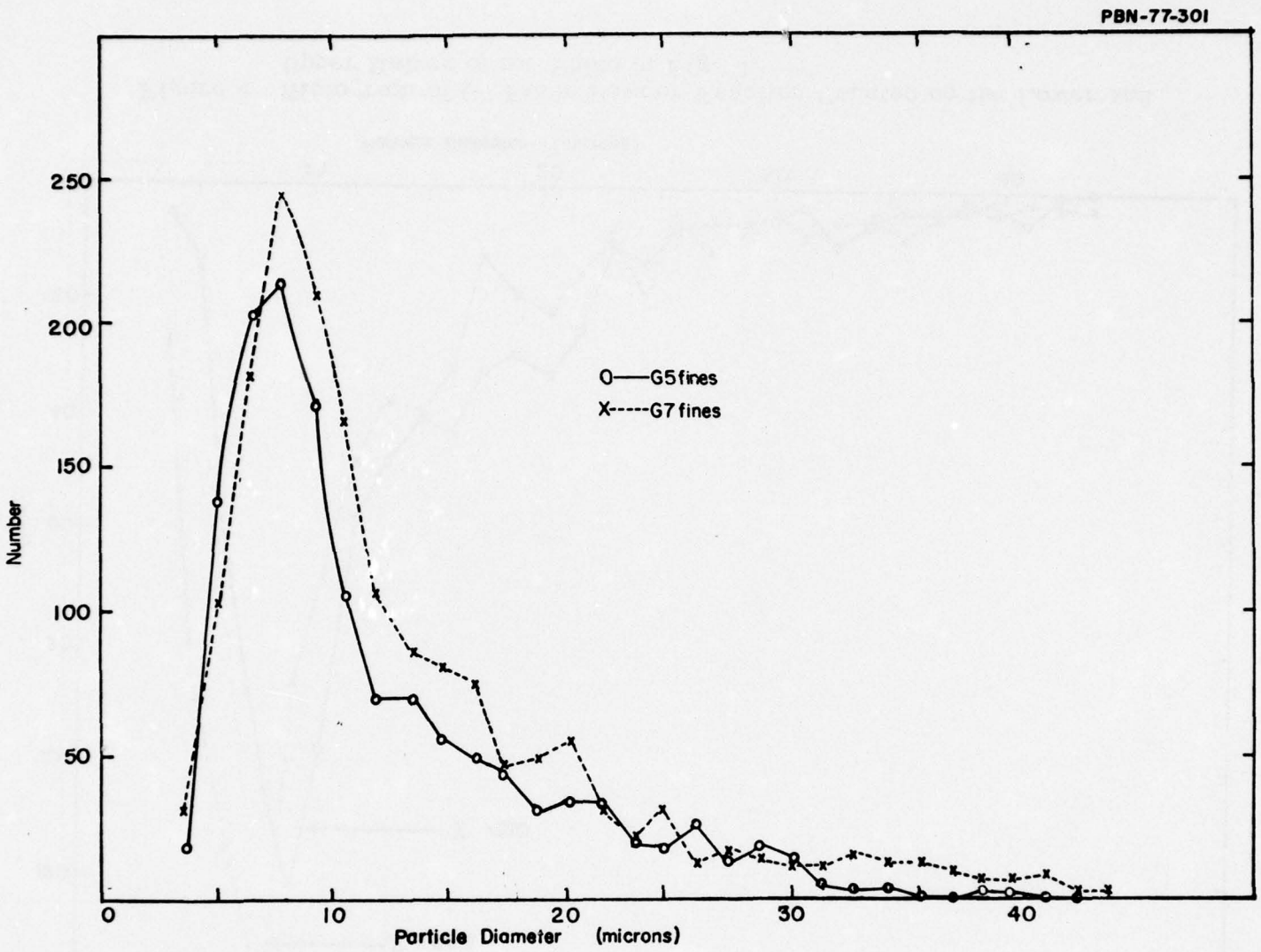

Figure 5 Particle-Size Histogram Graphing the LMTF475(G5) Fines Fraction Powder from Figure 2 and the LMTF475(G7) Fines Fraction Powder from Figure 3.

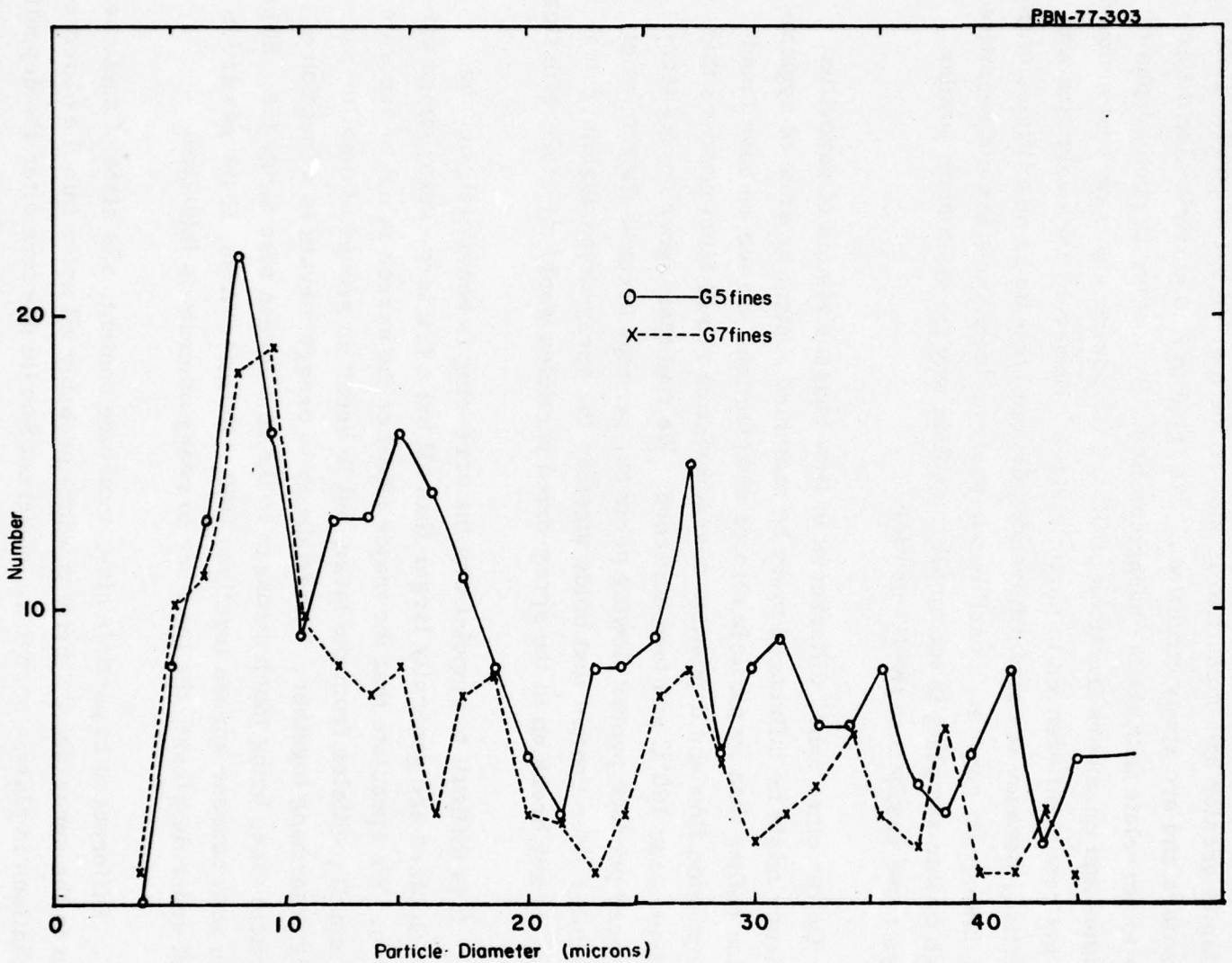

Figure 6 Histogram Graphing Particle-Size Distribution of the Smaller-Size Range of G5 and G7 Chambers Fractions.

Arc plasma runs with the G7 ferrite powder indicate flow characteristics that are adequate but not as good as the G5 powder. The tendency for clogging is greater and deposition is slower for a given set of powder flow parameters and arc spray conditions. We tried to find particle size differences to correlate with these characteristics. By looking at photographs of both fines and chambers fractions of G5 and G7 powders we saw what seemed to be noticeable differences in particle sizes. However, the evaluation was subjective, because the size differences did not show up as quantifiable changes in the histogram curves. Possibly our analysis techniques are not sensitive enough or our sampling is too small to explain why the G5 ferrite powder sprays more easily than the G7 powder.

On the other hand, differences in flow characteristics of deposition efficiency might be influenced more by moisture content or state of agglomeration rather than by particle size or distribution. So far we have found that optimum flow and deposition characteristics result from powders that are dried near 100°C and then screened. We find that higher drying temperatures produce poorer flowing powders, perhaps because they drive off the small binder content that holds together the spray-dried agglomerates. Certainly any break up in the spray-dried particles would interfere with flow.

It is difficult to pinpoint why the screening is beneficial, because screen sizes are generally larger than all but a few large spray-dried particles. We speculate that the major effect of the screen is not to separate the small particles from the large, but to break up groups of smaller particles that hang together. The tendency to reagglomerate is a function of particle size, being much stronger in the fine screen size range (50 - 80 μm) than with coarser screen fractions (100 - 200 μm). Also, if the powder is kept under dessicant, the tendency to reagglomerate is inhibited.

Differences in particle size, moisture content, and state of agglomeration in the spray-dried ferrite powders probably all enter into the observed variations in plasma spraying. Different ferrite powders alter the deposit rate anywhere from 20 to 50 percent, requiring changes in arc current and powder gas velocity - powder feed rate and other factors to optimize deposition. These adjustments in spray parameters require talent and ingenuity on the part of the operator.

2.2 APS Experiments at Raytheon

2.2.1 Equipment modifications

A new assembly for controlling motion of the substrate has been installed and tested. The metal support plate has been completed. The metal support plate and the pedestal motion assembly (Fig. 7) occupy extra space below the spray hood, necessitating a relocation of the spray hood, and a concomitant relocation of the hydraulic ram, the oil feed lines, and the velocity sensor.

The new equipment has performed quite satisfactorily over a dozen or so testing runs. Substrate wobble has not been eliminated, but its occurrence and severity have been reduced to the degree that we no longer expect to need the upper bearing to capture the free end of the substrate. This is fortunate because now we need not move the assembly in and out each time a sample is transferred to the holding oven and a new substrate was fitted in place.

We began experimental runs with the rebuilt, larger-volume spray chamber mentioned in the Sixth Quarterly Report. Four heating elements of Kanthal* resistance wire were built into the chamber side-walls, the two front elements operating on separate controllers and capable of a power output of 1500 W each. The two rear elements are operated at reduced power levels under manual (Variac) control. The resistance wire of each element was cement-coated to minimize interaction with the overspray powder.

The cement coating proved to be the source of heating-element failures, which resulted in considerable down time in the plasma spray program. Heater elements failed repeatedly after about 10 hours of operation where the chamber temperature was no higher than 750°C – a range well within the service temperature and watt density surface loading capabilities of the

---

* Trade name, Kanthal Corporation.

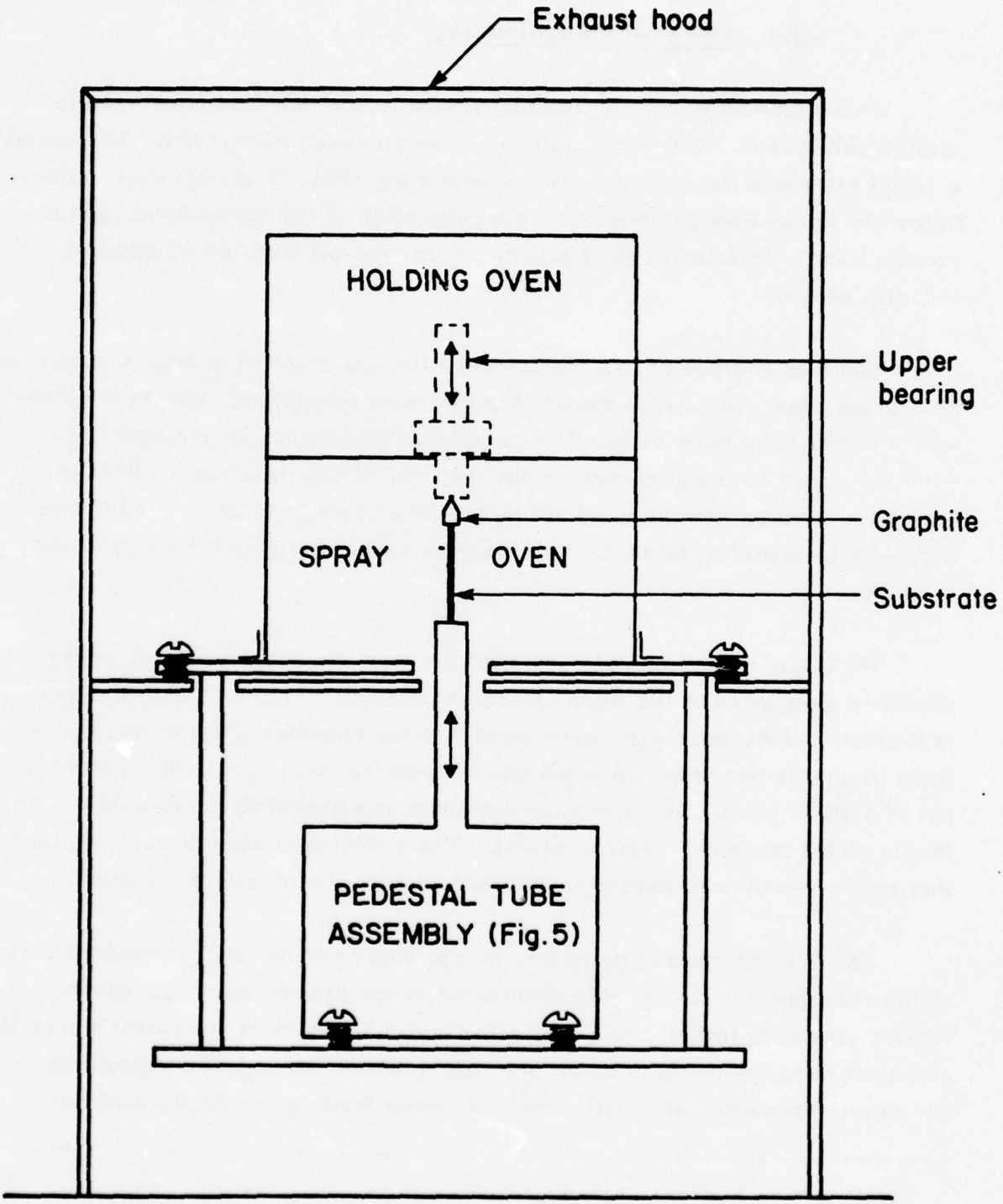

Figure 7 Diagram of Metal Supporting Plates and Interconnected Equipment

Kanthal wire. X-ray transmission photographs of the failed elements showed the cause of failure was widespread melting of the wire under the cement coating. Apparently the cement entrapped enough heat to induce melting (1400° C) without allowing sufficient radiation transfer into the furnace chamber. The manufacturer has supplied us with new elements that do not have a cement coating. We have made only a few runs with these elements, so it is too early to tell if the change has increased element life. The wire is recessed in grooves so that ferrite powder buildup is not too rapid, but it is clear that powder contamination will be more of a problem with uncoated units. We have adopted a "wait and see" attitude toward these modifications.

Our machine shop has designed a graphite cylindrical plug for holding the two-piece dielectric rod, which appears to be a significant improvement over the previous design. The earlier design was an arrangement of stainless steel jaws with a circular hole in which the substrate is clamped in an upright position during spraying. Oxidation of the graphite during the run does not pose any serious problems.

It is too early to tell if the graphite plug will prove more reliable than the steel jaw clamping assembly. The latter is being kept as a complete assembly, should we decide that the new arrangement is unsatisfactory.

2.2.2 Plasma spray runs and hysteresis preparations on machined samples

The first APS run with the newly enlarged spray chamber was made on January 6. The powder used, as shown in the Arc Plasma Log (Table I), was the LMTF475(G5) spray-dried powder; the dielectric had the nominal composition

$$Li_{1.0}Mn_{0.1}Ti_{1.0}Fe_{0.83}Al_{0.07}O_4$$

This is the dielectric to be used on the production run. The spray

TABLE I

ARC PLASMA SPRAY LOG
High Velocity Nozzle

Date	Number	Ferrite	Dielectric	Current Amps	Gas Flow-CFH Arc	Gas Flow-CFH Powder	Roto Feed Hopper Speed %	Spray Distance in	Rate Rot %	Rate Pull in/min	Furnace Chamber	Temp Holding	Anneal Cycle	Comment
1/6/77	297	LMTF 475 G-5 -88μ 60° Dry	LMTAF 201-7A	220	Ar35	$O_2$15	50	2 7/8	35	0.9	700	900-600	1015°(11)-2Hrs-O_2	Chamber deepened - New Elements - 2 Pair 550W - used
	298			220-240	35	15	50-60		35	1.0	715	650		
	299			240	35	13	60		F35R	1.0	700	650		Rotation reversed at midpoint
	300			220	35	15	50		35	1.0	700	650		
	301			230	35	15-20	50-60		60	1.0	715	650		Higher rotation to reduce substrate separation - ineffective
	302			240	35	15-20	50-60		48	1.0	715	650		
	303		NP*	235	35	20	60		45	1.1	725	650		Retainer clip shift appears to reduce substrate separation
	304		NP	235	35	20	60		45	0.95	725	650		
1/12/77	305	LMTF 475 G-5 -88μ 100° Dry	LMTAF 201-7A NP	230	35	15	50	2 7/8	45	0.9	650	650		
	306		NP	230	35	15-17	50		45	0.9	700	650	1015°(11)-2Hrs-O_2	Heavy substrate Breakage with Powder Gas Initiation
	307		NP	260-230	37	15	50		40	1.1-0.9	725	650		"Upper" Spray
	308		NP	230	35	15-12	50		40	0.95	710	650	1015°(11)-2Hrs-O_2	
2/10/77	309	LMTF 475 G-5	LMTAF 200(4)	310-280	35	25	55	3 3/8	50	0.85	650	600		First Run with Mounting Tube Indirect Drive Assembly and Suspension Plate- Tube jaws not tight enough on substrate- Powder not dry enough New Tube Drive works well
	310			280	35	20	55		50	0.85	650	600		
	311			280	38	20-25	50		35	1.0	710	600		
	312			400	Shut down because of poor deposit conditions									
2/16/77	313	LMTF475 G-5 -88μ	LMTAF 200(4) NP	250	43	20	50	2 5/8	45	1.0	685	600	1015°(11)-2Hrs-O_2	First use of graphite substrate base and modified new mounting tube
	314		NP	250	43	20	50		45	1.0	700	600		
	315		NP	250	38	20	55-50		35	1.0	700	600		Substrate separating upon initiation spray
	316		NP	250	38	20	50		45	0.85	700	600		

* No preheat (NP)

TABLE I (Cont'd.)

ARC PLASMA SPRAY LOG (Cont'd.)
High Velocity Nozzle

Date	Number	Ferrite	Dielectric	Current Amps	Gas Flow-CFH Arc	Powder	Roto Feed Hopper Speed %	Spray Distance in	Rate Rot %	Pull in/min	Furnace Chamber	Temp Holding	Anneal Cycle	Comment
2/21	317	LMTF475 G-5 -88μ	LMTAF 200(4) NP*	260	38	15	50		40	1.1	700	600		
	318		NP	240	38	15	50-55		45	1.1	720	600		
	319		LMTAF 201-7A NP	220	38	15	55		45	1.05	725	600		Tube reject rod malfunctioned
	320		NP	200	38	14	55-50-60		45	1.1-0.9	725	600		Increased overspray exhaust with heat reduction
	321		NP	220	38	13	50		45	1.0	725	600		Best run parameters for day
	322		NP	220	38	15-10	70-60		45	1.2	600	600		
	323		NP	220	38	13	60		45	1.3	600	600		Substrate half cracked
3/8	324	LMTF475 G-7 -88 +53μ	LMTAF 200(4) NP	270	35	15	70	2 5/8	50	1.5	780-740	600	1015^{0}(11)-2Hrs-O_2	After oven conditioning @ 100% particle size 10%-88u +53u, 60%-53μ +44, 30%-44u. Powder flowing eratically. First use of G-7 powder and uncoated elements in this series
	325		LMTAF 200-7A NP	210-220	35	20	70-65		50	1.3	760	600		
	326		NP	240	35	20	60-65		50	1.2	760-770	600		
3/9	327	LMTF475 G-7 -88 +53μ dried at 100° 4 hrs then screened	LMTAF 202-7A NP	260	35	16	65		50	1.4	725	600		
	328		NP	240	38	15-20	60		50	1.1	760-725	600		
	329		NP	220	38	20-25	60		45	1.0	725-755	600		220 amps appears to be minimum for powder parameters - current fluctuating at flow of 35 CFH
	330		NP	280	35	20	60	3.0	45	0.9	735-760	600		
	331		NP	240-250	38	20	60	2 5/8	45	1.0	730-740	600		
	332		NP	260-270	38	20	50	2 5/8	45	1.0	745-765	600		Overspray reduced with hopper speed reduction
3/11	333	LMTF475 G-7 -53 + 44μ	LMTAF 202-7A NP	270-320	38	17-30	50-65		45	1.0	730	600	1015^{0}(11)-2Hrs-O_2	G-7 powder flow erratic at best, but hopper gas leak may be the cause
	334		NP	320	38	30	65		42	1.0	730	600		
	335		NP	320	38	30	65		45	1.2-1.1	730	600		
	336		NP	320	38	30	65		42	1.1	730	600		
	337		NP	350	38	30	65		45	1.1-1.0	730-745	610		Current crept up from 320 - 360
	338		NP	320	38	30	65		45	1.1-0.8	730	600		Conditions poor - hopper leak severe - Graphite plug wobbly

* No preheat (NP)

parameters were 220 amps arc current and 15 CFH powder gas velocity, typical of conditions used in the confirmatory run. The as-sprayed boules shown in the Appendix were uniformly coated and fairly straight although the wall thickness after final machining is not ideally uniform. APS 298 was essentially a repeat of 297 at a slightly higher arc current. In sample 299 the rotation direction was reversed at midpoint to determine its effect on deposit rate. The deposit rate did, in fact, increase as can be seen in the X-ray photo in Appendix A. In subsequent work we have found that the dependence of deposition rate on rotation direction is one of several factors that can influence the ferrite coating thickness. The dependence is caused by the fact that the ferrite deposit pattern is heavier to the right of center when viewed from behind the gun. During spraying the hot spot on the substrate tends to move with the sense of rotation. If this spot moves into the heavier spray zone of the unsymmetric spray pattern, the deposit rate will increase. Deposit rate is also sensitive to other factors such as concentricity of substrate rotation and spray chamber temperature.

Samples APS 300 to 304 were sprayed under nearly identical conditions. Efforts were made to reduce the separation between substrate halves by increasing rotation rate and changing powder feed velocity. These changes were not as effective as moving the retainer clips another half inch closer together. It appears that substrate separation will continue to be a factor in reproducibility until one-piece dielectrics are developed.

Table II shows the coercive force (H_c) and remanent magnetization (B_r) at 15-amp turns obtained on the samples in this series which went through the various production steps.

Samples 305 to 308 in Table II were sprayed again with G5 powder but with some experimentation on direction of translation and introduction of substrates without preheating (marked NP in Table I).

TABLE II

HYSTERESIS PROPERTIES OF APS

Samples 297 to 304

APS No.	H_c	B_r	Comments
297	2.50	728	
298	2.29	774	
299	--	--	Broke during spray
300	2.45	730	
301	3.16	763	
302	--	--	Broke in machining
303	3.32	725	
304	--	--	Too short

The next APS run on February 10 was the first with the new rotation translation equipment, still using the steel jaws to clamp the bare substrate rod. Results were rather poor because the jaws were not holding the substrate securely. APS runs 309 to 312 did not yield worthwhile samples.

On February 16 we first used a graphite plug arrangement for holding the dielectric, hoping that this new assembly would simplify the process of sample transfer. The graphite plug, about 0.75 in. diameter has a slight taper which is matched by a similar taper in the receiving hole in the pedestal tube. Since the substrate is fitted in a slightly undersized center hole, there is no problem of wobble due to misorientation of the dielectric in the holding mechanism. There is some problem with oxidation in the holding (600°C) oven after spraying which limits the reuse of the graphite plugs, but the greater ease in transfer outweighs the added cost. The samples APS 313 to 316 were not worth further processing because of the experiments with the new assembly.

On February 21 another APS run was made using the graphite plugs and dielectric rods of type LMTAF200(4) and LMTAF200(7A). The hysteresis properties on this series are summarized in Table III.

TABLE III

HYSTERESIS PROPERTIES OF APS SAMPLES 317 to 324

APS No.	H_c	B_r	Comments
317	2.84	719	
318	2.25	803	
319	--	--	Cracks in boule
320	2.04	805	
321	1.92	617	
322	2.10	707	
323	--	--	Failed during spray

The series APS 320, 321, and 322 were particularly interesting in this series because spray conditions were nearly identical and samples were machined sequentially and annealed together. X-ray photographs were taken of the machined phase shifters (Appendix A) and very careful measurements of wall thickness were made on these three. An examination of these three photographs shows that there was bowing in APS runs 321 and 322 which qualitatively agrees with the order of remanent magnetization (B_r) if we invoke the argument that wall nonuniformity reduces B_r by a similar percentage. Table IV gives the percentage decrease in ferrite wall uniformity which, according to our physical model, should reduce the overall B_r by a similar percentage. Assuming $B_r = 850$ for a perfectly uniform toroid, the second column gives a calculated B_r assuming wall nonuniformity is the only factor reducing B_r. The third column repeats the measured B_r at 15 amp-turns drive and the fourth and fifth indicate the microwave properties of differential phase shift and insertion loss that were measured on APS 320 and 322.

From the calculated and observed B_r it is clear that the degree of nonuniformity correlates with remanence but the change is stronger than the simple linear relationship. The percentage drop in B_r is nearly twice the

percentage decrease in wall thickness in each of the three cases. It is of course also possible that other unknown factors further reduce B_r but they do not change the order dictated by wall thickness. We note that the arc current was quite low (200-220 amps) in these three runs, so that overheating is probably not the cause of warping.

TABLE IV

CALCULATED AND OBSERVED B_r AND MICROWAVE PROPERTIES ON APS SAMPLES

APS No.	Uniformity (%)	Calc. B_r	Obs. B_r	$\Delta\Phi$	Ins. Loss
320	96.7	822	805	395	0.44
321	88	759	617	--	--
322	91	774	707	342	0.57

The spray runs on March 8, March 9, and March 11 were carried out with the graphite holder and the new rotation – translation equipment. The dielectric was the LMTAF200(7A) material where, x = 1.0 and y = .07 in $Li_{.5+x/2}Mn_{.10}Ti_xAl_yFe_{2.4-3x/2-y}O_4$. The ferrite powder was the new batch of LMTF475(G7) described in Sec. 2.2.2. The spray procedure had been changed in that the dielectrics were not preheated but placed directly on the pedestal tube through the open door of the holding oven. We have had no evidence of thermal shock using this procedure. The spray conditions are summarized in the Arc Plasma Log, Table I. The arc current was maintained at 250-280 amps in the first two runs, but was increased in the last to raise the deposition rate, which had been falling off (apparently because of a leak in the powder hopper). The setting at 45 percent in this series corresponds to 100 rpm sample rotation rate.

Samples APS 327 and 329 in Table V were bowed 0.009 in. and 0.011 in. which produced wall nonuniformities and reduced B_r. Another contributor to reduced B_r was the lack of a final 800°C anneal for these samples and APS 331.

TABLE V

HYSTERESIS PROPERTIES OF APS SAMPLES 324 - 332

APS No.	H_c	B_r	Comments
324	--	---	Warped
325	3.10	775	Coating separation near top warped, no 800° anneal
326	--	---	
327	3.26	535	
328	3.57	760	
329	3.11	427	Warped, no 800° anneal
330	3.04	760	
331	3.21	754	No 800° anneal
332	3.26	760	

APS samples 333 through 338 were not processed in time to give any magnetic property data.

2.2.3 Test results on confirmatory samples

A total of 20 samples were tested in accordance with the requirements for first article inspection on this contract and delivered with a report on January 27, 1977.

The plasma spray conditions used to produce the phase shifter elements are summarized in Table VI. Six of the early samples (APS 161, 162, 163, 176, 241, and 244) made use of ferrite powder with slightly lower $4\pi M_s$ ($\sim$1200 gauss) but otherwise identical with the higher $4\pi M_s$ ($\sim$1230 gauss) G5 powder used for the remaining runs. We have found that the choice of dielectric composition, within the narrow limits of composition and resulting expansion coefficient ($\bar{\alpha}_{1000°}$), has little effect on the magnetic properties. The effect is probably finite but within the noise level of other factors such as spray conditions and uniformity in wall thickness. Two of the samples

TABLE VI

SPRAY CONDITIONS FOR CONFIRMATORY SAMPLES

(MIL-STD 831, Para. 5.6.10.1.4)

Sample Number	Ferrite	Dielectric	$-\alpha_{diel.}$ (ppm/°C)	Arc Gas Current (amps)	Arc Gas Flow (cfh)	Carrier Gas Flow (cfh)	Spray Distance (in)	Pull Rate (in/min)	Spray Chamber Temp. (°C)
161	50(G4)	200(7A)	15.4	290	36	17.5	3.25	1.0	700
162	50(G4)	200(7A)	15.4	290	36	17.5	3.25	1.0	700
163	50(G4)	200(7A)	15.4	290	36	17.5	3.25	1.0	700
176	50(G4)	180(33)	14.7	300	36	17.5	3.25	1.1	700
225	475(G5)	180(33)	14.7	320	38	25	3.25	0.7	680
234	475(G5)	200(2)	15.6	390	40	20	3.25	0.7	700
238	475(G5)	190(15A)	14.7	320	38	22	3.25	0.8	750
241	50(G4)	195(10A)	14.9	320	38	22	3.25	0.75	625
244	50(G4)	195(10A)	14.9	320	38	25	3.25	0.8	670
264	475(G5)	200(4)	15.1	360	40	25	3.25	0.9	700
270	475(G5)	200(4)	15.1	200	35	10	2.87	1.0	680
274	475(G5)	200(4)	15.1	210	35	12	2.87	1.1	700
277	475(G5)	200(4)	15.1	210	35	12	2.87	1.0	650
279	475(G5)	200(4)	15.1	210	35	12	2.87	1.0	690
281	475(G5)	200(4)	15.1	210	35	10	2.87	1.0	680
282	475(G5)	200(4)	15.1	210	35	10	2.87	1.3	700
286	475(G5)	201(7A)	15.4	210	35	11	2.87	1.1	700
289	475(G5)	201(7A)	15.4	220	35	13	2.87	1.1	700
291	475(G5)	201(7A)	15.4	220	35	12	2.87	1.0	710
293	475(G5)	201(7A)	15.4	220	35	14	2.87	1.3	710

(APS 176 and 275) are slightly shorter (0.030 in.) than the desired length due to machining errors. These samples were included because they meet all of the contract specifications for full-length elements.

For sample runs through APS 264, the spray distance was 3.25 inches. Arc currents of 290-360 amperes and carrier gas velocities of 15-25 CFH were used. Beginning with APS 270, samples were made at 2.87 in. distance, the minimum practical spray distance for our equipment. The latter spray distance permitted a reduction in arc current (210-220 amperes), arc gas flow (35 CFH), arc gas, and powder gas flow (10 - 15 CFH). Faster pull rates were made possible by the increased deposit efficiency at the reduced spray distance. The spray chamber was kept at about 700°C and the upper holding oven at 650°C during spraying.

The incidence of cracking in machined and annealed phase shifters decreased to very low levels in the more recent samples. This is attributed to the improvements in spray technique, which allow uniform ferrite coatings in both the radial and longitudinal directions. Samples were given the standard anneals at 1015°C, 2 hours in O_2 in as-sprayed condition, and 800°C, 2 hours in air after machining for stress relief.

The hysteresis loop and microwave property measurement results are summarized in Table VII, and the temperature variation data on 10 phase shifters are shown in Table VIII. Twenty samples were tested for B_r and H_c, and 10 of these were given further waveguide testing.

The confirmatory test procedure calls for temperature dependence of H_c and B_r as well as microwave measurements on the same 10 samples. In normal scheduling this would call for hysteresis and microwave testing on the first 10 (that is, APS 161 through APS 270). However, we felt that the tests should be performed on some of the latest samples, where incremental improvements in technique and materials were constantly taking place. Because of time limitations, we did not succeed in focusing all tests on the latest 10, but did succeed in testing five (APS 274 through APS 282).

TABLE VII

CONFIRMATORY SAMPLE TEST RESULTS
(MIL-STD 831, Para. 5.6.10.1.4)

			Loop Properties							RF Properties at 5.45 GHz									
			25°C		- 30°C		+ 85°C				25°C			- 30°C			+ 85°C		
APS No.	W.G. Phase Shift	Temp. Meas.	H_c (Oe)	B_r (g)	H_c (Oe)	B_r (g)	H_c (Oe)	B_r (g)	$\frac{\Delta B_{r\,T}}{B_r}$	Length (in.)	$\Delta\phi_{(o)}$	$I\phi_{(o)}$	I.L. dB	$\Delta\phi_{(o)}$	$I\phi_{(o)}$	I.L. dB	$\Delta\phi_{(o)}$	$I\phi_{(o)}$	I.L. dB
161		x	3.13	649	3.87	675	2.60	591	± 6.6	5.145									
162		x	3.02	636	3.60	665	2.55	576	± 7.2	5.145									
163	x		2.84	636						5.145	346	3732	1.0						
176	x		3.12	686						5.114	355	3711	1.4						
225	x		2.32	715						5.115	366	3646	0.7						
234	x		2.75	725						5.145	400	3715	1.88						
238			2.45	680						5.145									
241	x		2.68	733						5.145	371	3760	1.1	477	3687	1.4	315	3829	1.2
244		x	2.70	754	3.30	805	2.22	665	± 9.5	5.145									
264		x	2.84	767	3.33	808	2.28	682	± 8.1	5.145									
270		x	2.43	734	2.80	779	2.05	660	± 8.3	5.145									
274	x	x	2.84	733	3.52	777	2.47	666	± 7.7	5.145	383	3636	0.60	454	3430	1.0	318	3755	.3
277	x	x	1.85	753	2.15	808	1.64	660	± 10.1	5.145	380	3668	1.38						
279	x	x	2.85	770	3.35	796	2.43	711	± 5.6	5.145	416	3720	1.20						
281	x	x	2.53	789	3.43	830	2.12	730	± 6.4	5.145	410	3658	0.58						
282	x	x	1.46	869	1.80	929	1.22	804	± 7.2	5.145	423	3671	0.60						
286			2.39	771						5.145									
289			2.67	792						5.145									
291			2.91	739						5.145									
293			2.99	748						5.145									

TABLF VIII

HYSTERESIS LOOP PROPERTIES vs TEMPERATURE

(MIL-STD 831, Para. 5.6.10.1.4)

Toroid No.	H_c (Oe)						B_r (gauss)						$\frac{\Delta B_r T}{B_r}$
	-30°C	-10°C	0°C	25°C	50°C	85°C	-30°C	-10°C	0°C	25°C	50°C	85°C	
161	3.87	3.52	3.52	3.13	2.84	2.60	675	660	659	649	630	591	± 6.6
162	3.60	3.52	3.32	3.02	2.75	2.55	665	655	651	636	611	576	± 7.2
244	3.30	3.01	2.84	2.70	2.47	2.22	805	787	781	754	722	665	± 9.5
264	3.33	3.24	2.99	2.84	2.54	2.28	808	793	787	767	736	682	± 8.1
270	2.80	2.66	2.55	2.43	2.21	2.05	779	763	754	734	710	660	± 8.3
274	3.52	3.36	3.15	2.84	2.73	2.47	777	763	754	733	705	666	± 7.7
277	2.15	2.13	2.06	1.85	1.79	1.64	808	792	781	753	719	660	±10.1
279	3.35	3.19	3.00	2.85	2.84	2.43	796	787	787	770	749	711	± 5.6
281	3.43	2.84	2.80	2.53	2.31	2.12	830	815	812	789	769	730	± 6.4
282	1.80	1.74	1.66	1.46	1.35	1.22	929	909	900	869	845	804	± 7.2

Again, for temperature dependence of the microwave properties, only one of this latest group (APS 274) could be tested in time. The other phase shifter for microwave temperature-dependence testing was APS 241.

All of the samples with the marginal exception of APS 277 (Table VIII) fell within the expected range of less than ± 10 percent variation in B_r. Table VII indicates that the later samples had somewhat higher phase shift ($\Delta\Phi_o$) and all were greater than the 340° required.

Insertion phase was measured on each of the rf tested samples. For a phased array phase-shifting element, the insertion phase in itself is of little importance. What is important is the variation of insertion phase from element to element. To measure this quantity, $\Delta I\phi$, the reference arm length was readjusted so that, with the reference phase shifter in place, we had again a near-zero phase indication over the frequency range (condition for equal electrical length of both arms).

The guideline goal of ± 16° was not achieved; the standard deviation for the 10 samples was 41.26° with a total spread of ± 48° about a mean value of 36.92°. The deviation is about 30 percent higher than the value obtained on several thousand PATRIOT elements installed in test antennas. One possible cause of the greater variation in APS phasers is the separation between halves of the two-piece dielectric. Another is the fact that dielectric and ferrite composition did vary slightly between early and later samples (see Table VI). In the later series of five the insertion phase grouping is much closer.

Insertion loss measured on APS samples was typically > 1 dB. Larger values were recorded, for example, in APS 234, where I. L. = 1.88 dB. Further annealing under oxidizing conditions reduced the value to ~ 1 dB in this particular sample. We conclude that the intrinsic loss for these elements is > 1 dB and that longer oxidation anneals would bring all samples into this range.

3.0 CONCLUSIONS

The primary activities of the seventh quarter were the testing and delivery of the 20 confirmatory samples and the redesign, rebuilding and testing out of improved rotation-translation equipment and holder assemblies.

The confirmatory sample testing was completed and a formal report submitted in January. The twenty samples passed all of the requirements, although phase shift was somewhat better on samples sprayed near the end of the confirmatory run. The average value was $\Delta\Phi = 384°$, with a standard deviation of 26.8. Insertion loss was typically less than 1 dB except for samples where annealing time was insufficient. We surmise that annealing time for the oxidation process which reduces insertion loss is critically dependent on ferrite density. We have changed from 2-hour to 4-hour anneals to assure low insertion loss.

After shipment of the confirmatory samples, the rebuilding of the APS equipment was completed. The basic objectives were to have the pedestal-motion equipment firmly tied into the furnace assembly, so that no relative shift in position could occur, and to rework the rotation-translation assembly so that no eccentric motion or error in position reproducibility could be due to equipment error. These objectives were met quite well as shown by subsequent test runs.

4.0 PROGRAM FOR THE NEXT INTERVAL

The confirmatory samples were tested at ECOM Laboratories and the results forwarded to us on March 22. The results showed good agreement in hysteresis loop properties and in microwave test data with Raytheon's report.

We have set up a test program beginning on May 1 extending to July 30 to make the necessary measurements on the 200 production samples. The spray schedule calls for 40 samples in April, 80 in May and 80 in June.

5.0 IDENTIFICATION OF PERSONNEL

The personnel who contributed to this production development effort during the seventh quarterly reporting period, and the manhours worked by each is shown below. Biographies of these personnel have been supplied in previous quarterly reports.

Name	Hours
J. Green	7
J. Van Hook	277
L. Lesensky	11
O. Guentert	21
D. Massé	20
R. Maher	369
Other	635
Total	1340

Appendix A

X-Radiography of Plasma-Sprayed

Boules 297 - 338

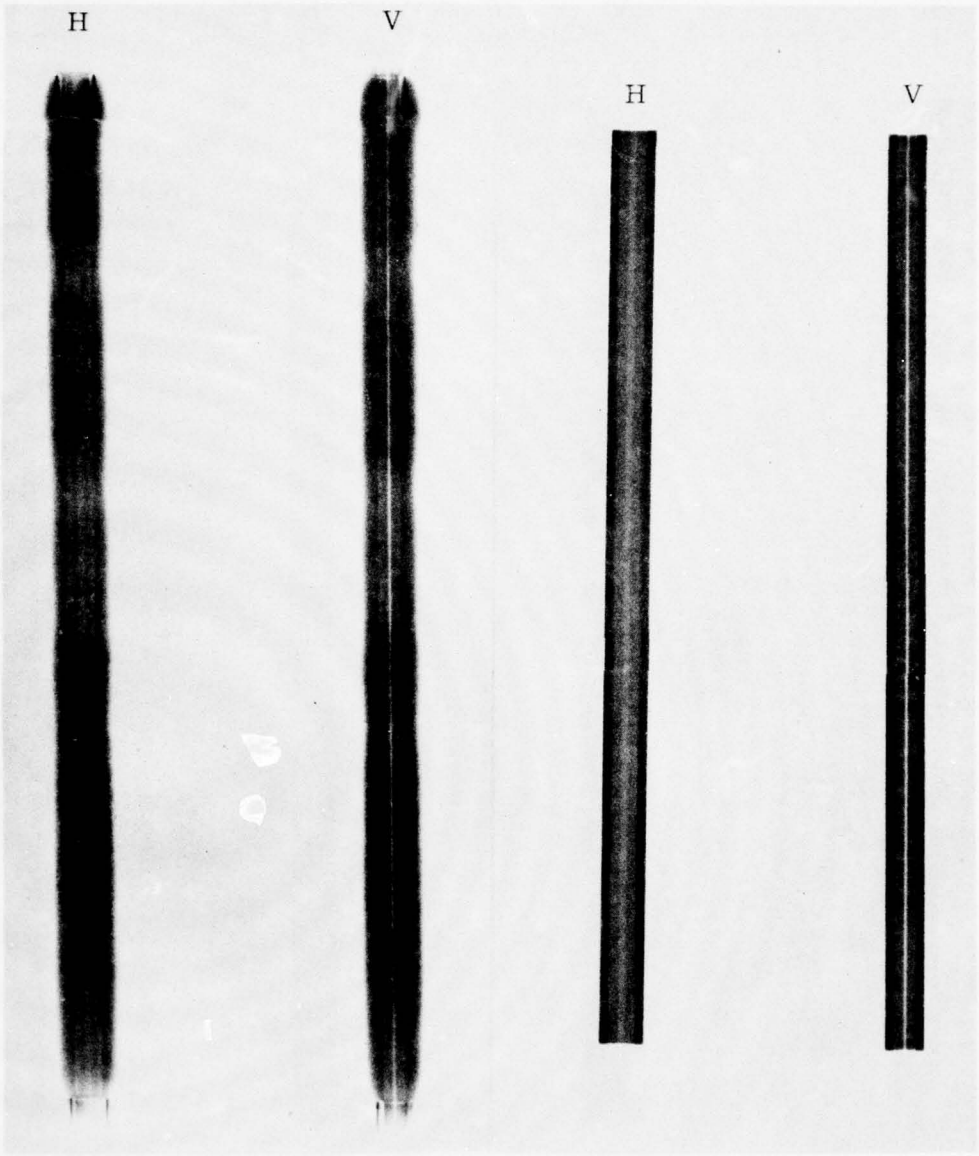

Sample No. 297

H V H V

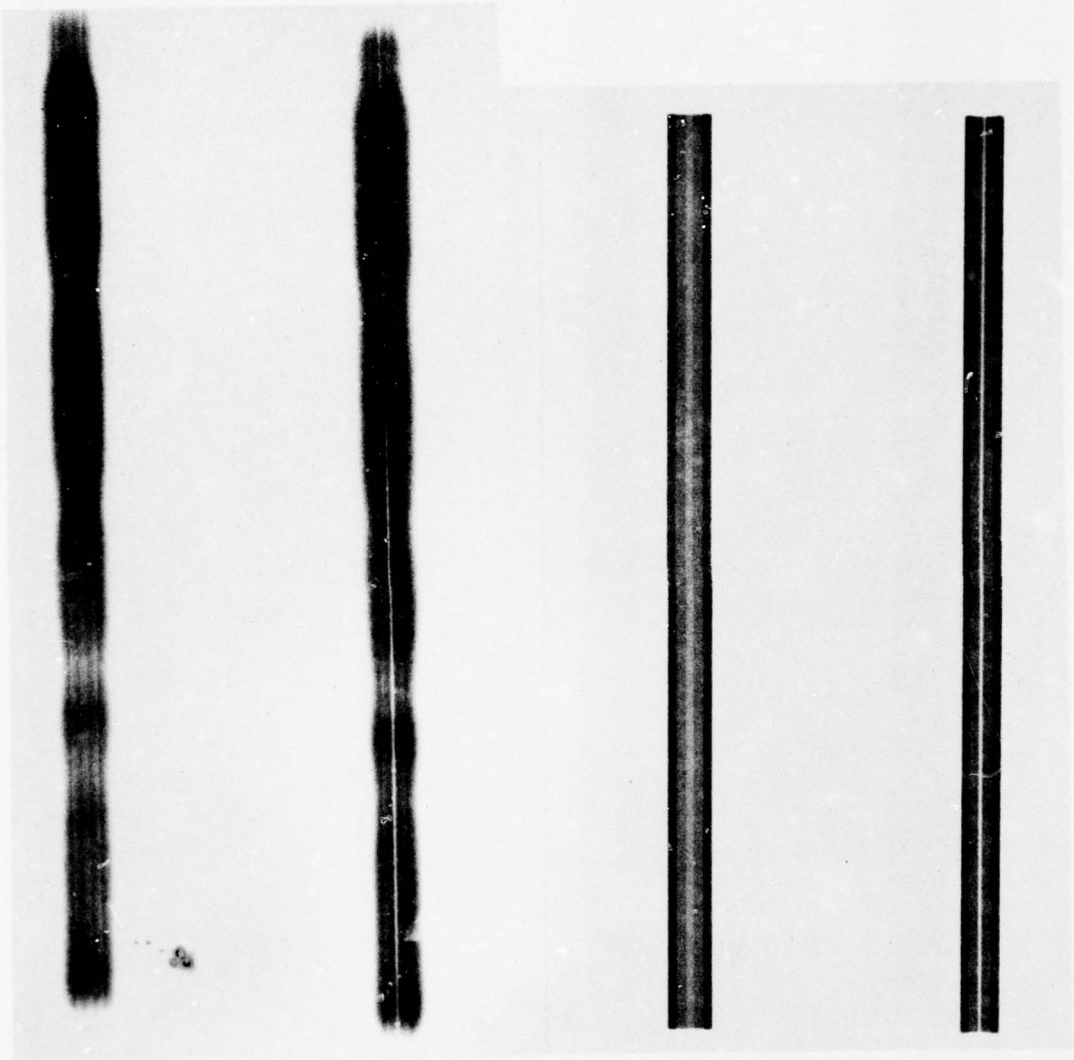

Sample No. 298

H V

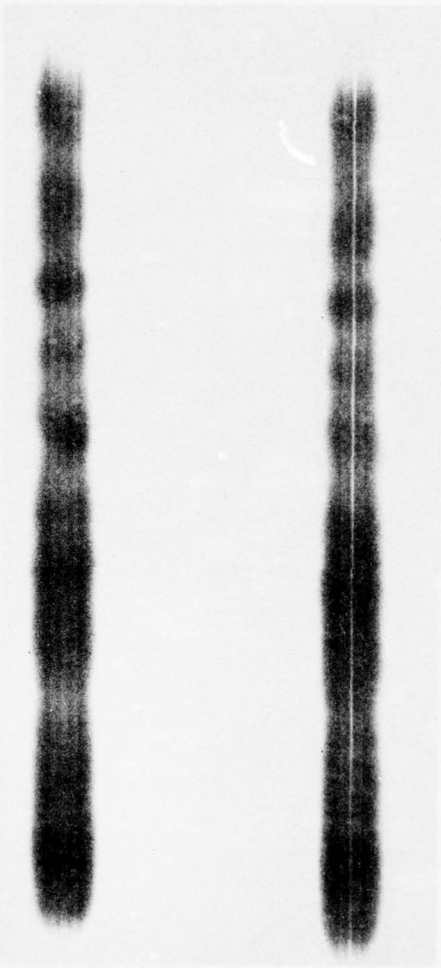

Sample No. 299

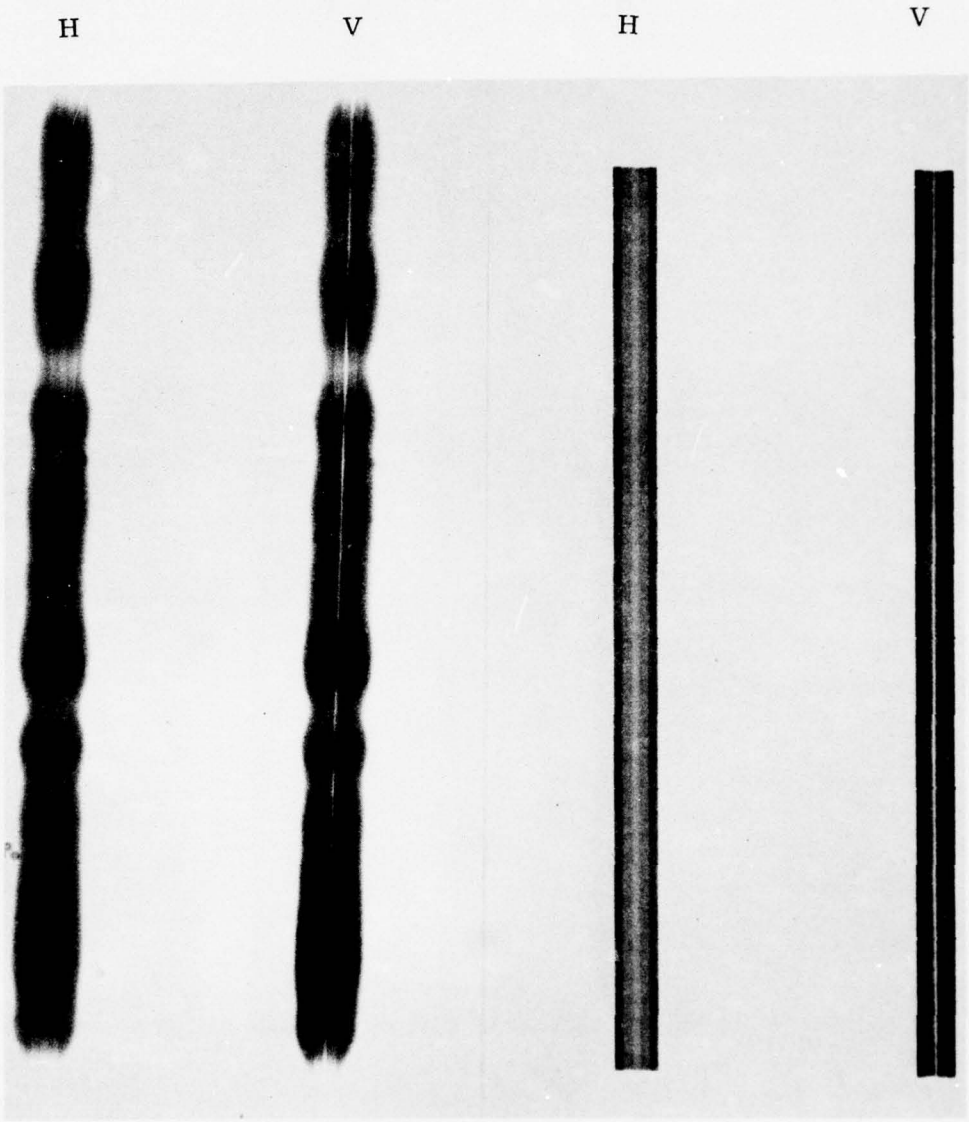

Sample No. 300

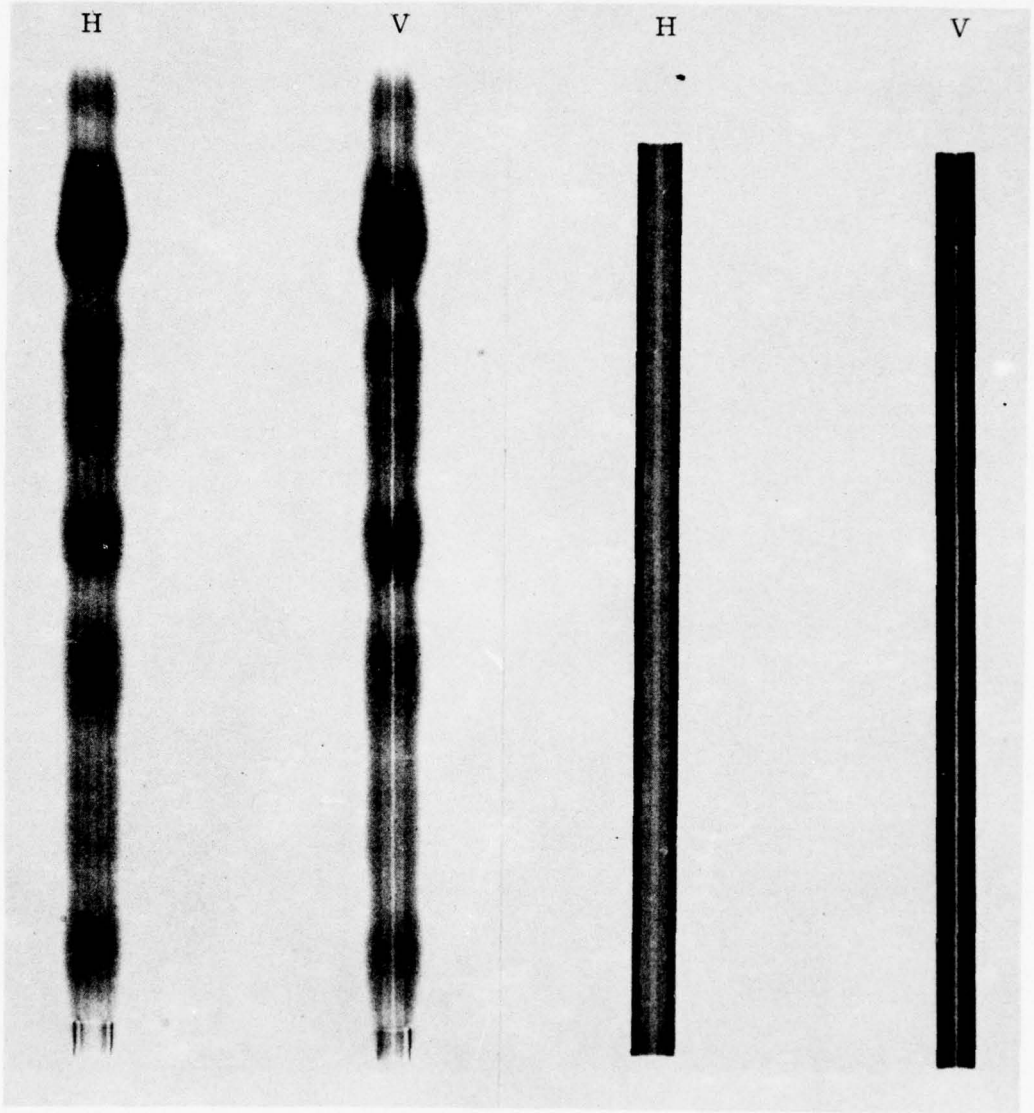

Sample No. 301

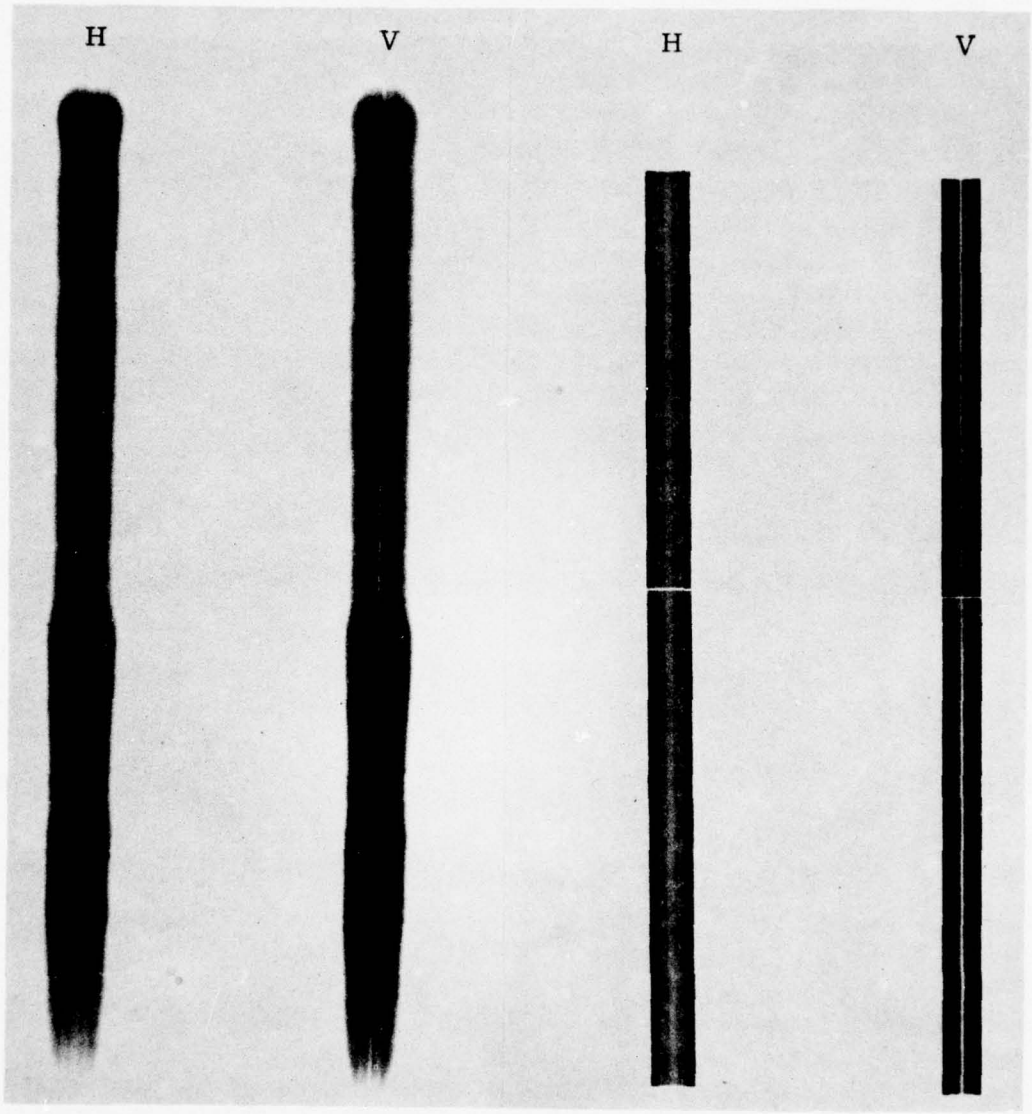

Sample No. 302

H V H V

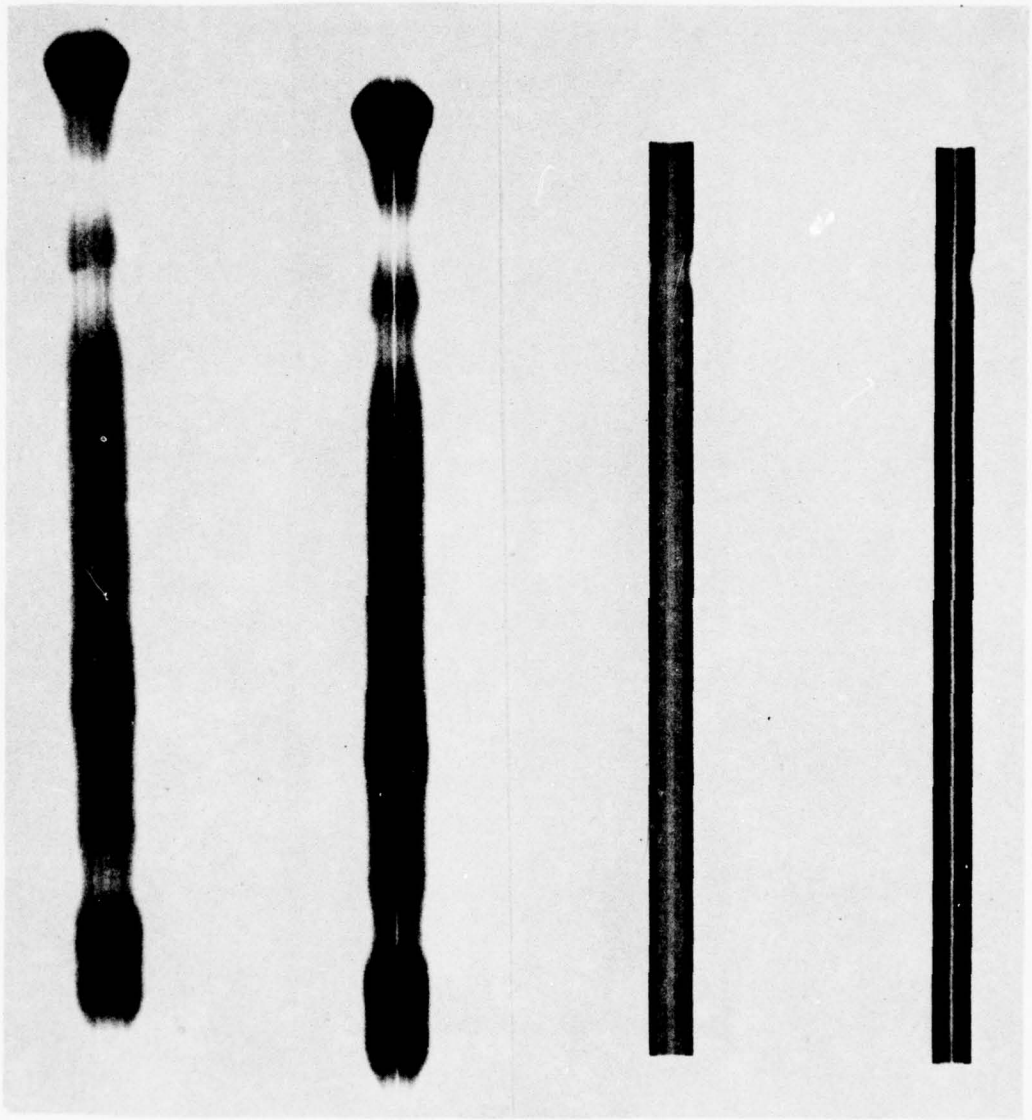

Sample No. 303

H V

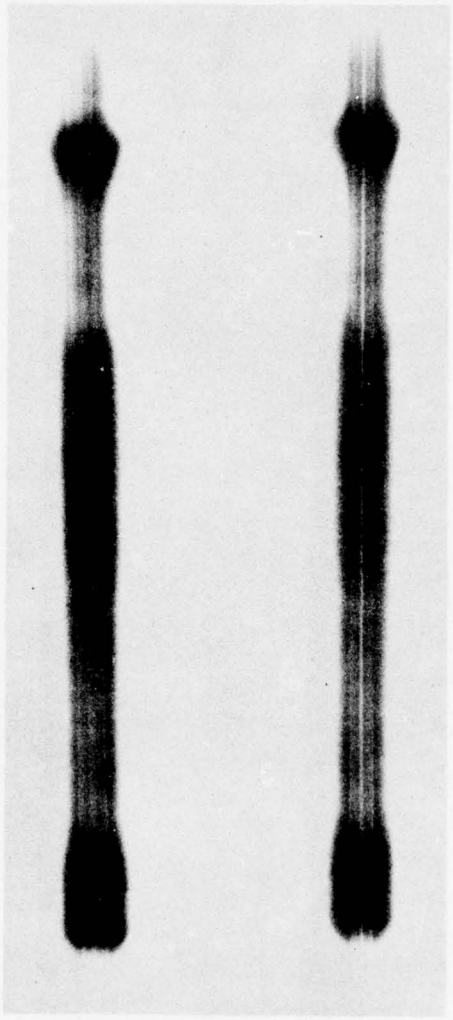

Sample No. 304

H V

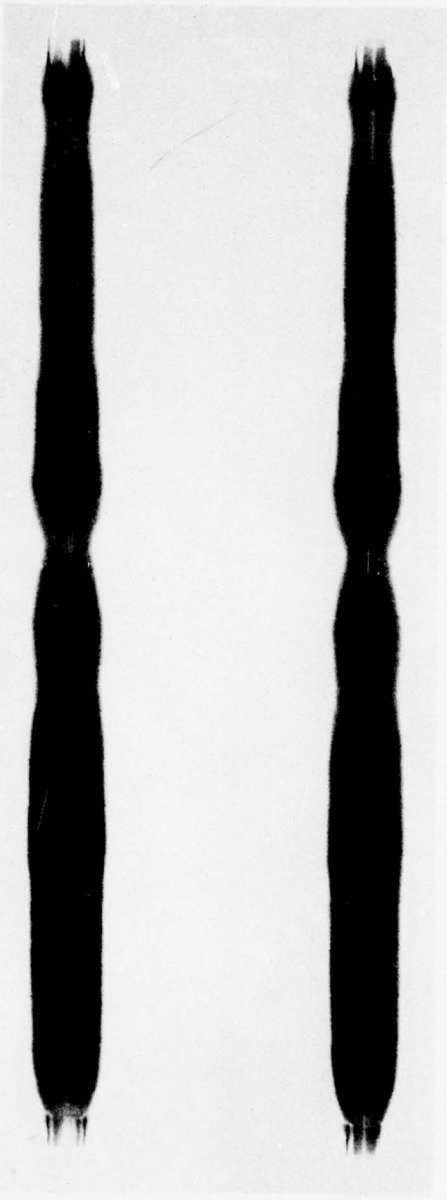

Sample No. 310

H V

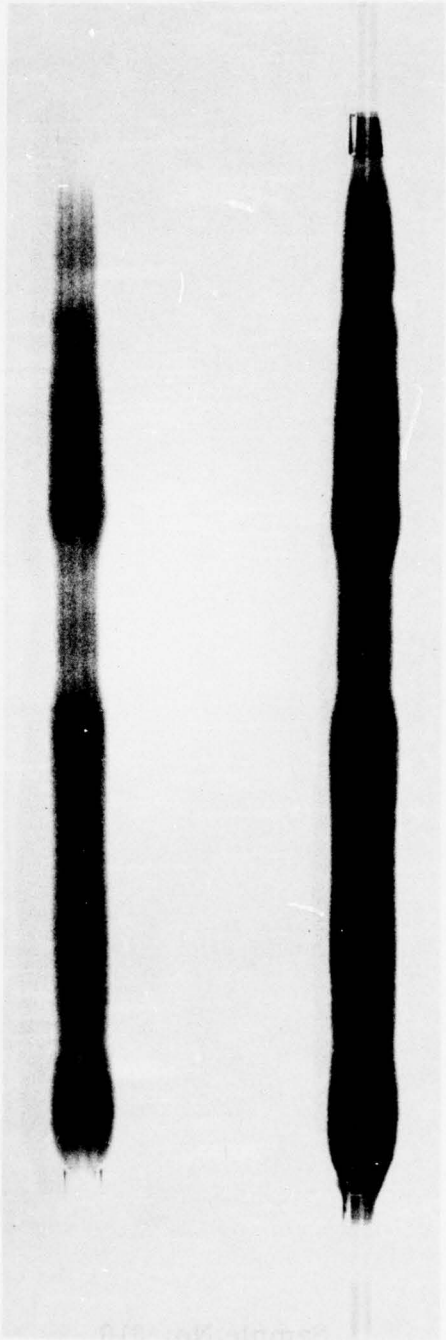

Sample No. 312

H V

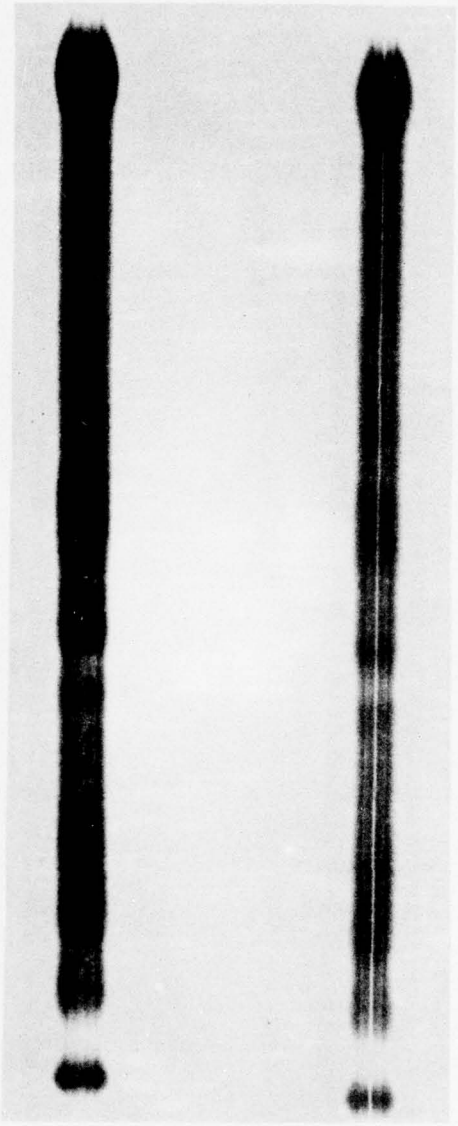

Sample No. 313

H V

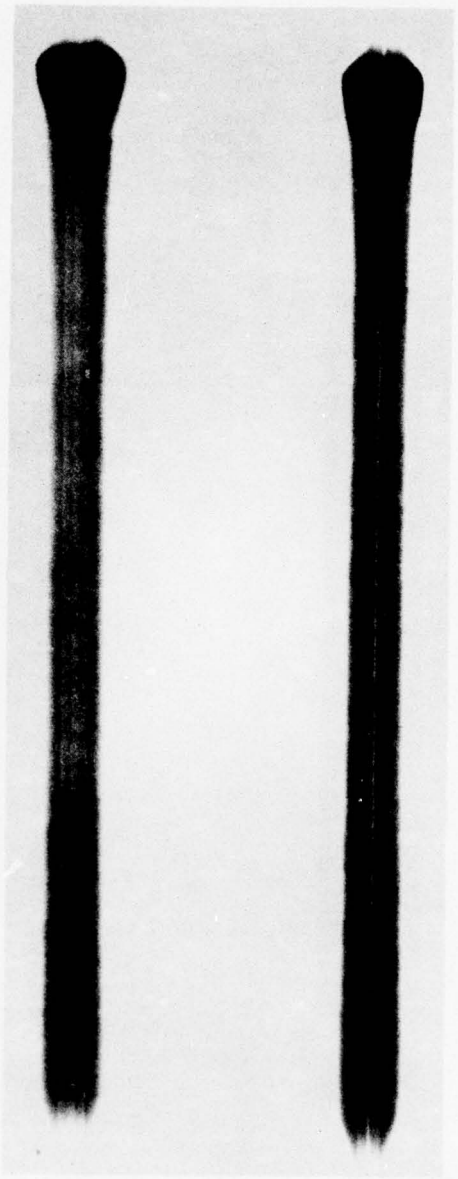

Sample No. 314

H V

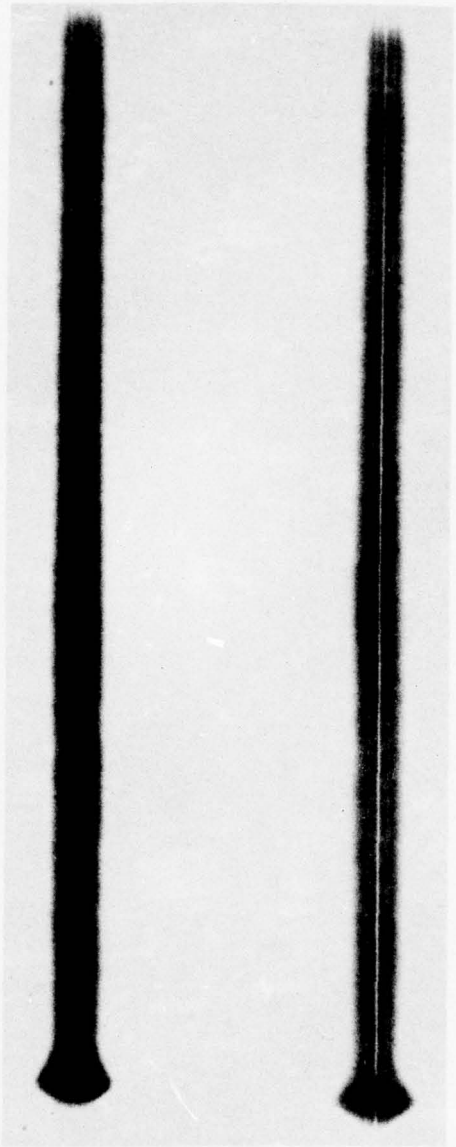

Sample No. 315

H V

Sample No. 316

H V

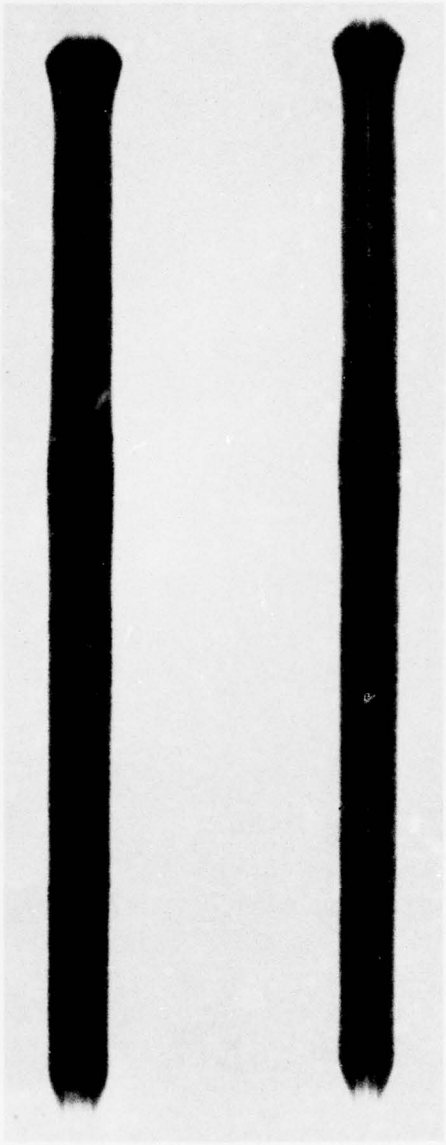

Sample No. 317

H V

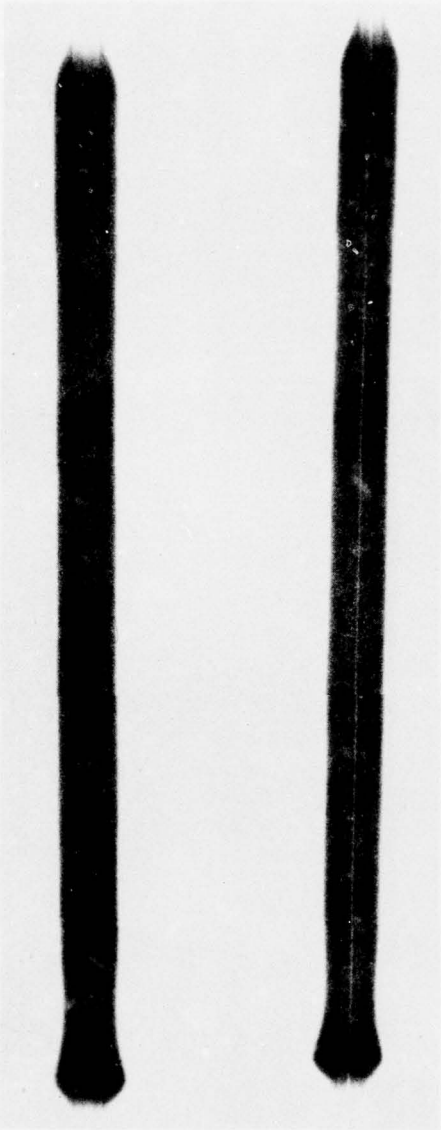

Sample No. 318

H V

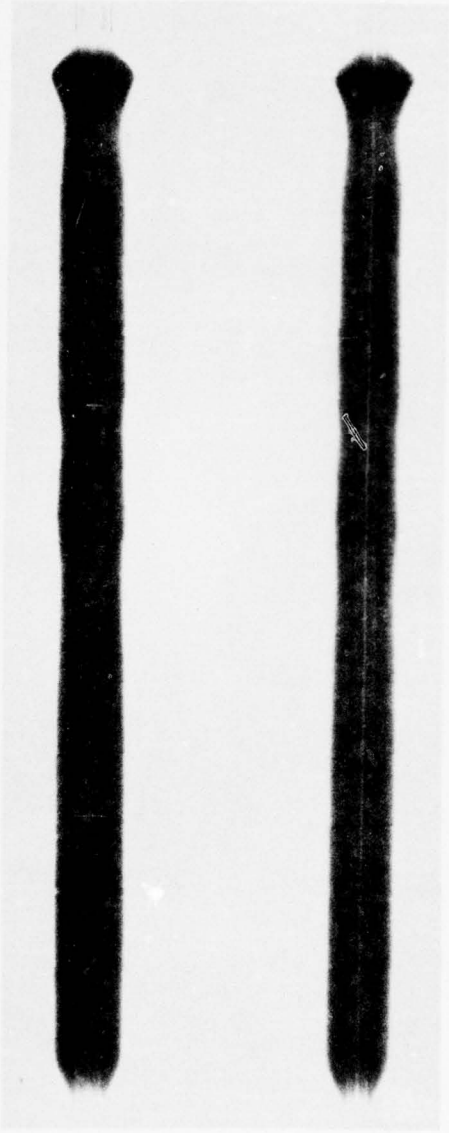

Sample No. 319

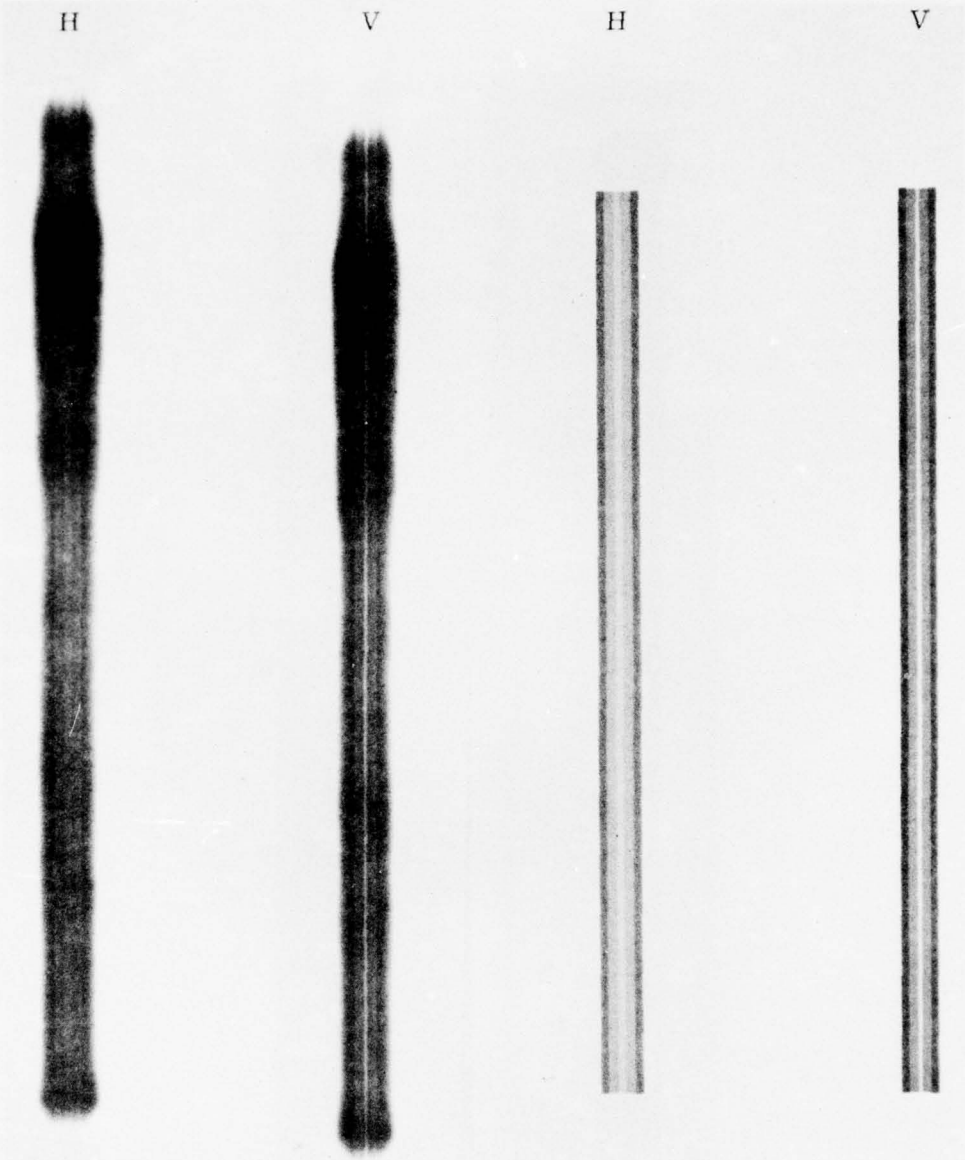

Sample No. 320

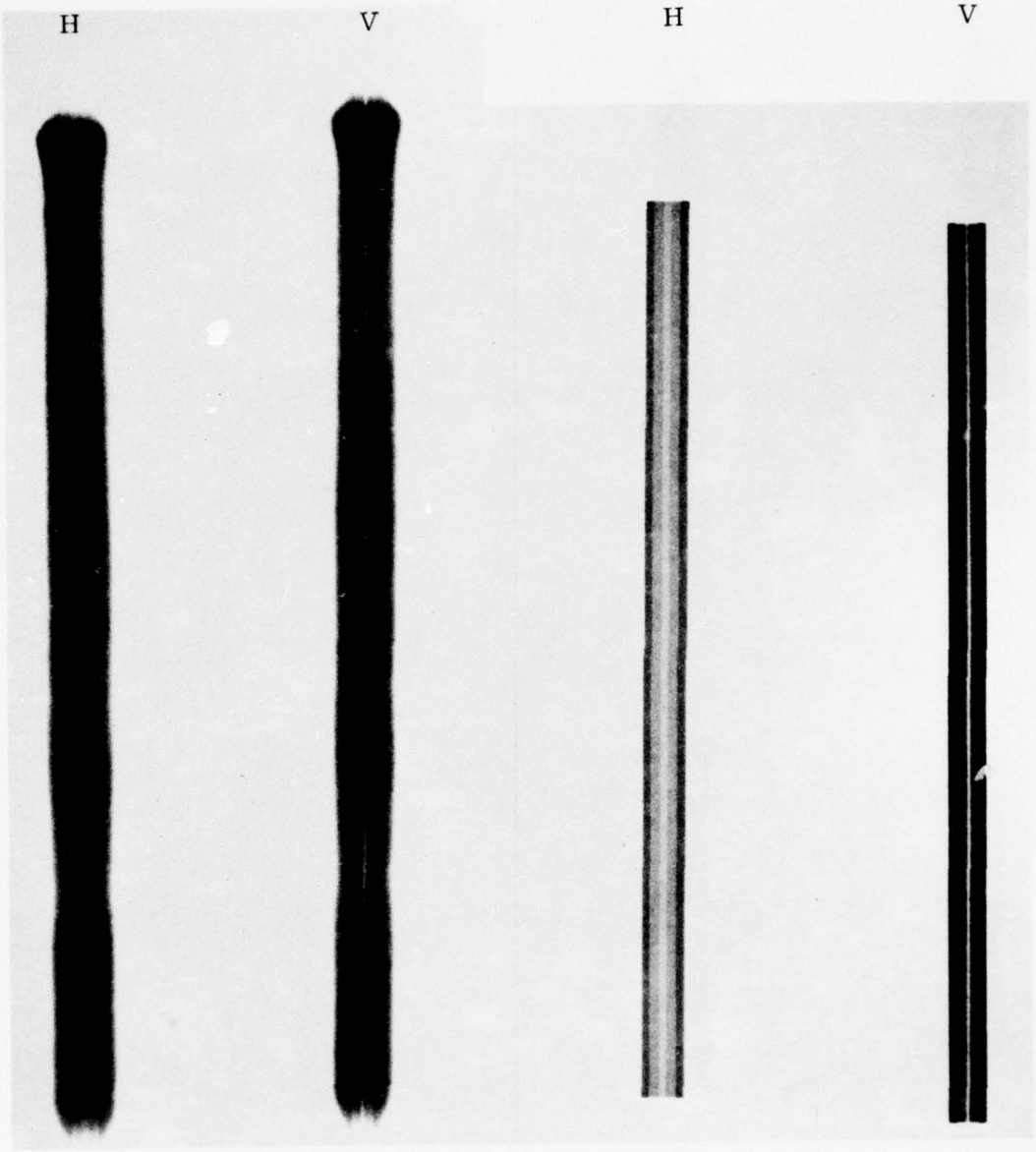

Sample No. 321

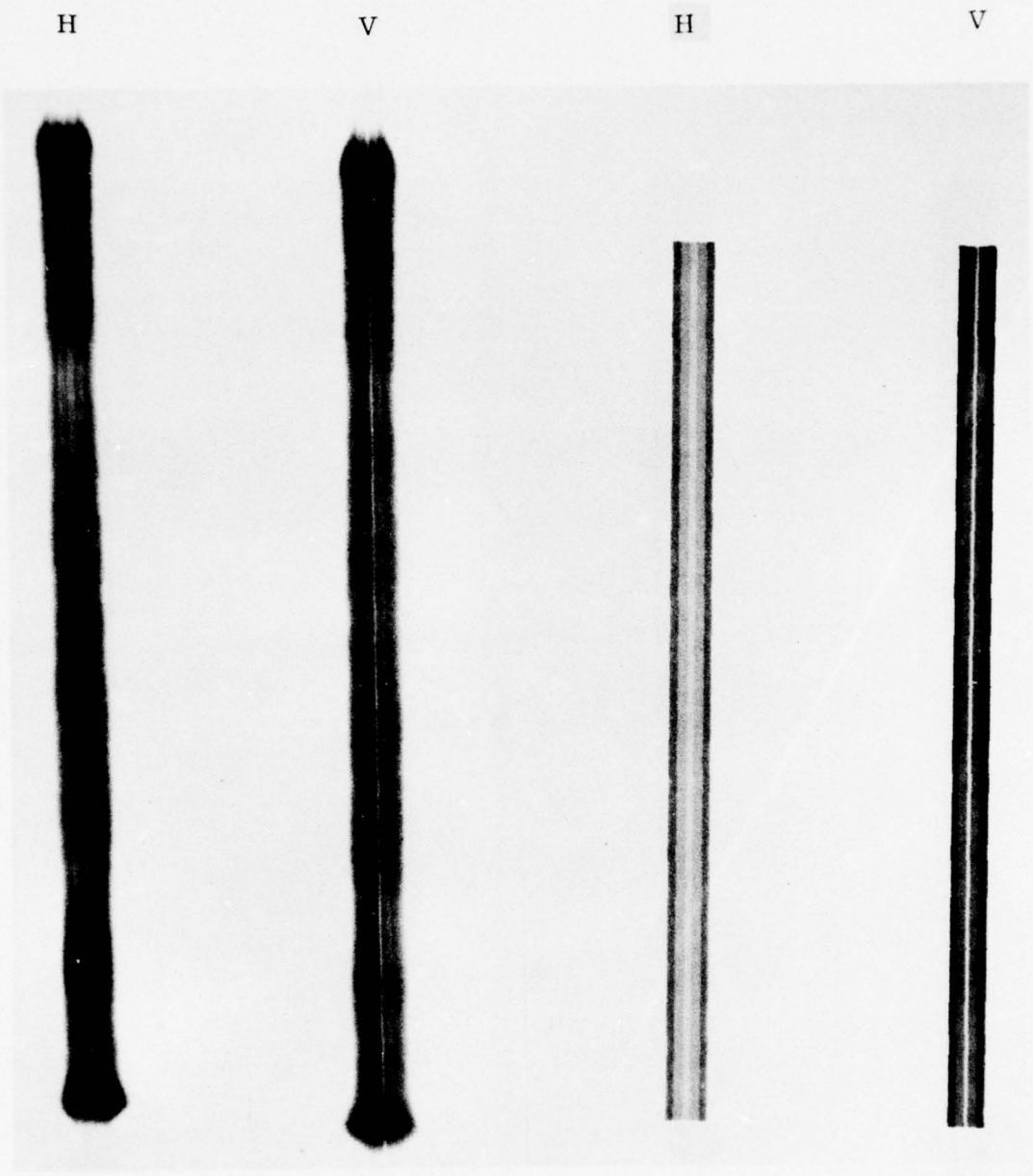

Sample No. 322

H V

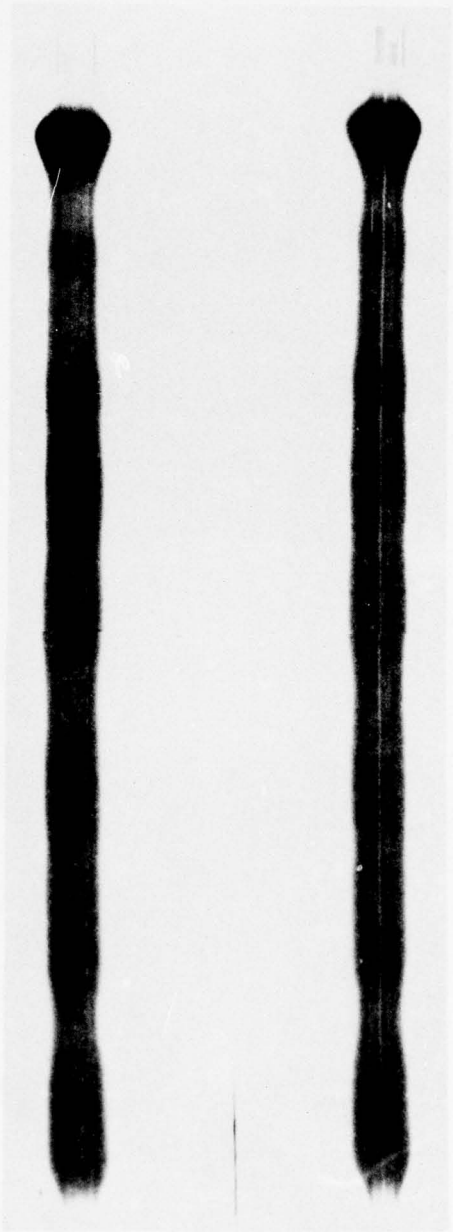

Sample No. 324

H V

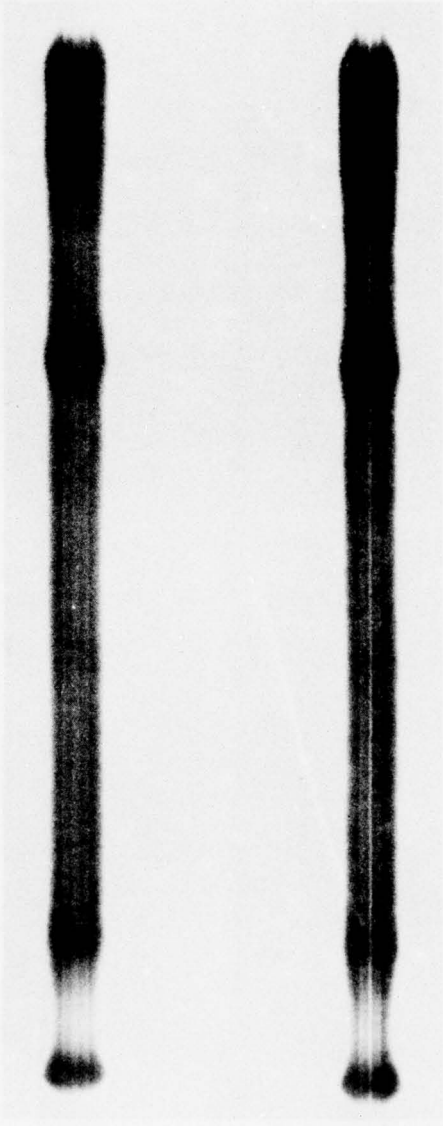

Sample No. 325

H V

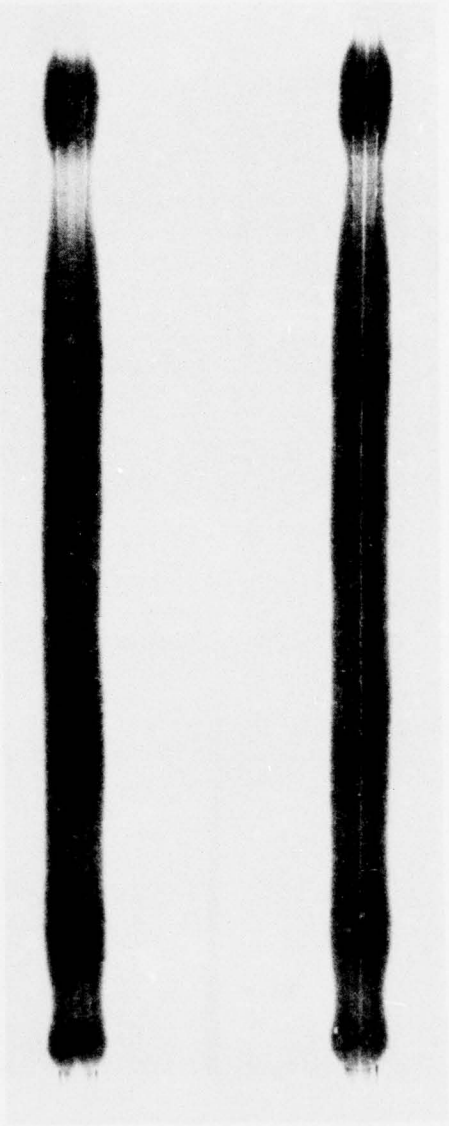

Sample No. 326

H V

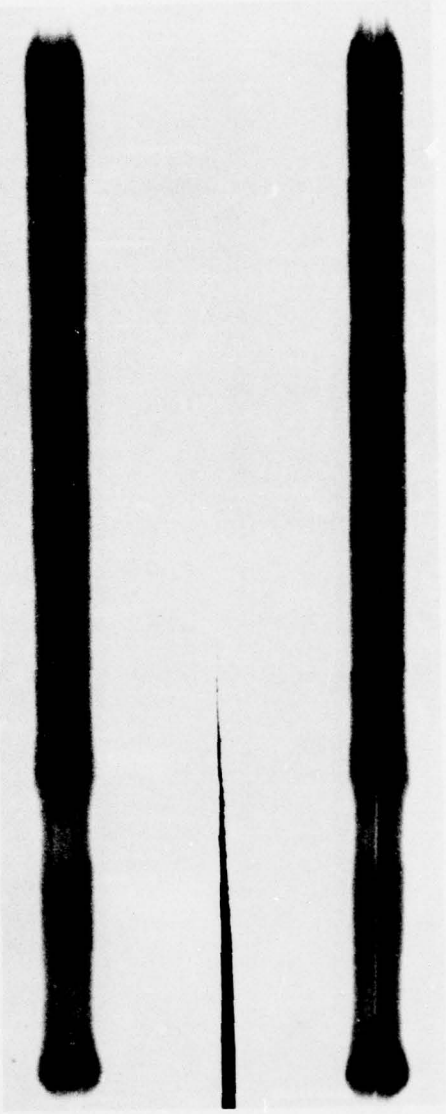

Sample No. 327

H V

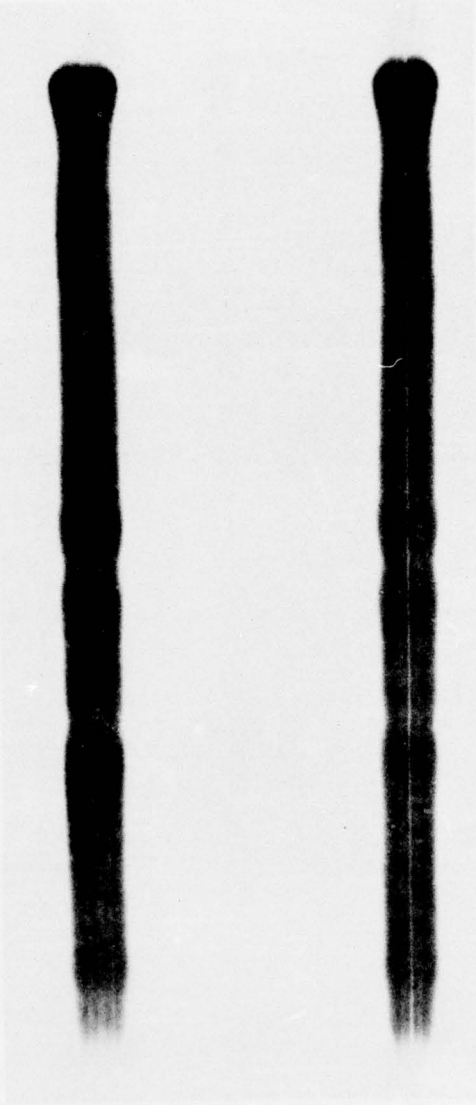

Sample No. 328

H V

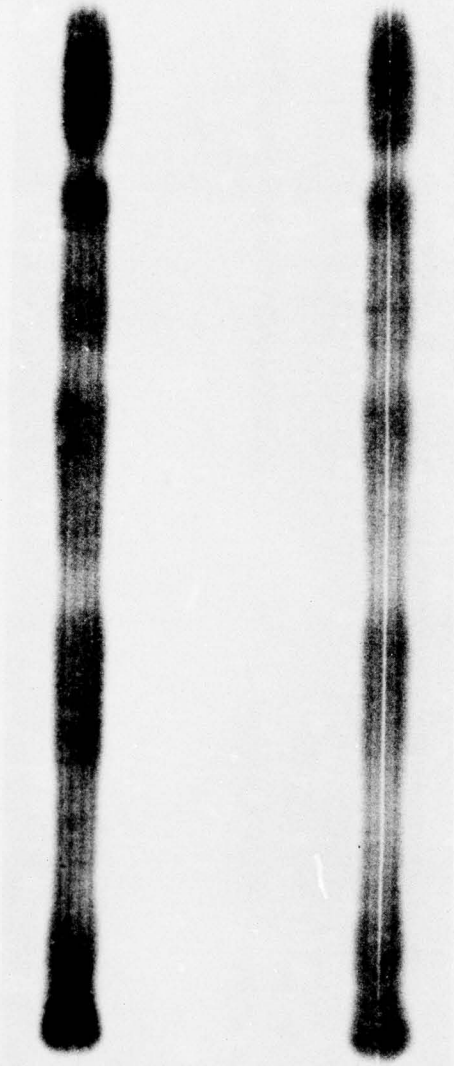

Sample No. 330

H V

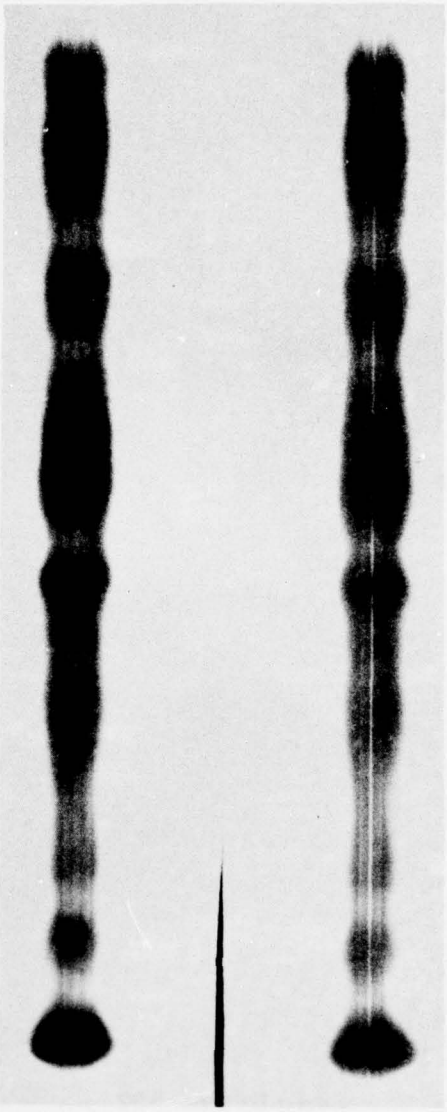

Sample No. 331

H V

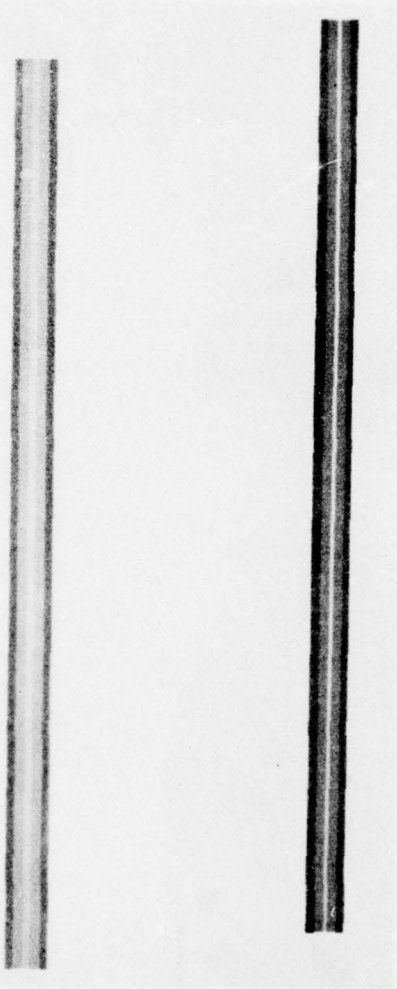

Sample No. 332

H V

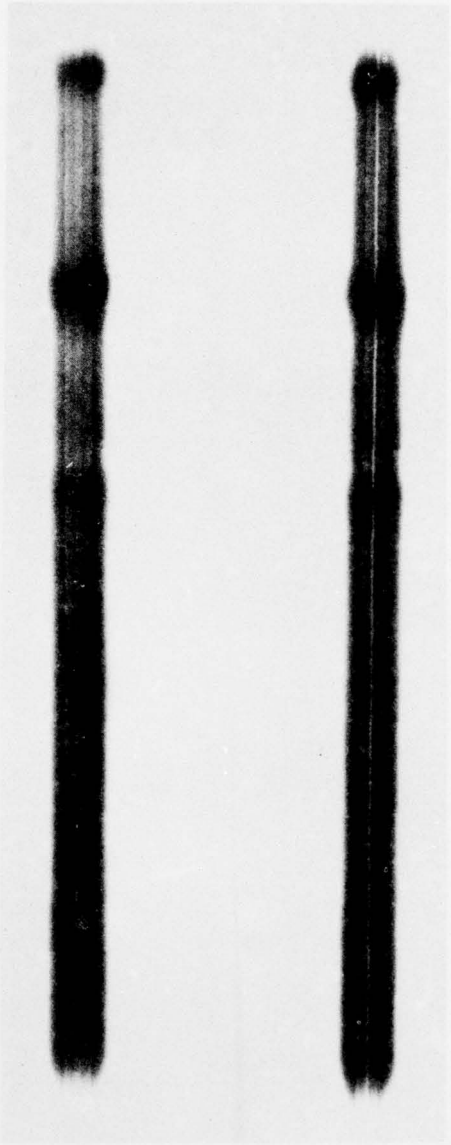

Sample No. 333

H V

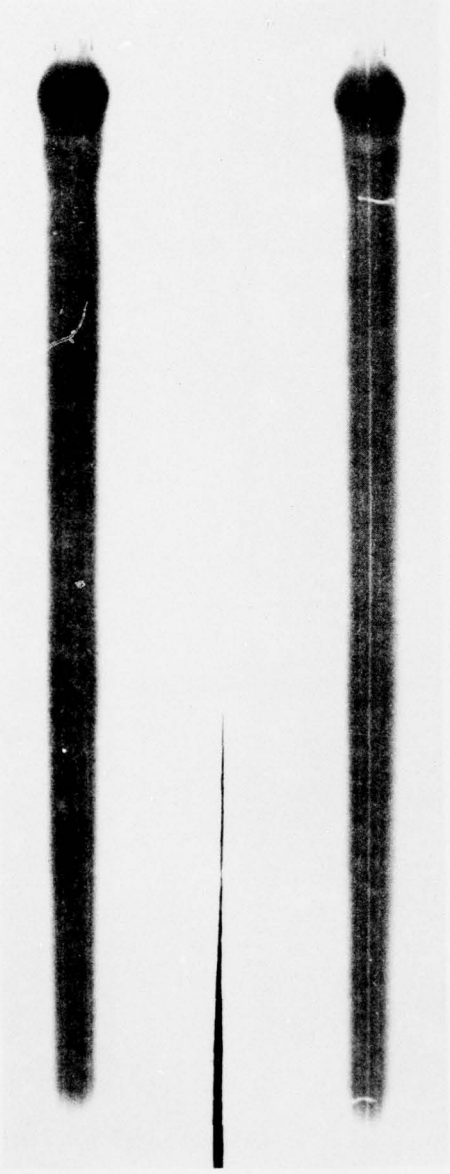

Sample No. 334

H V

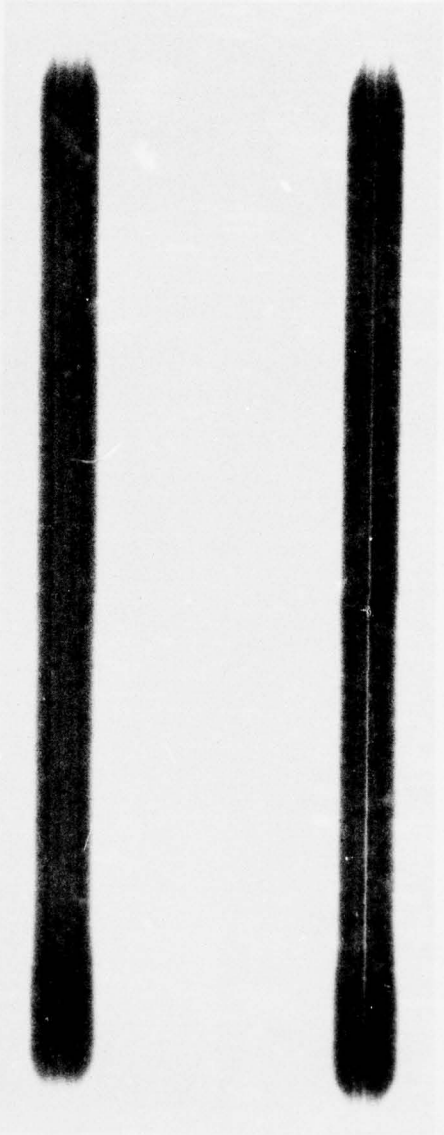

Sample No. 335

H V

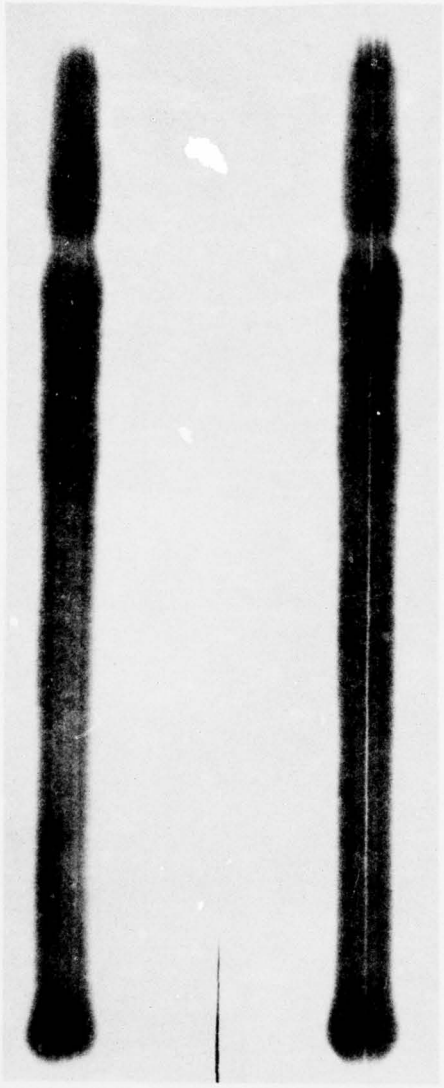

Sample No. 336

H V

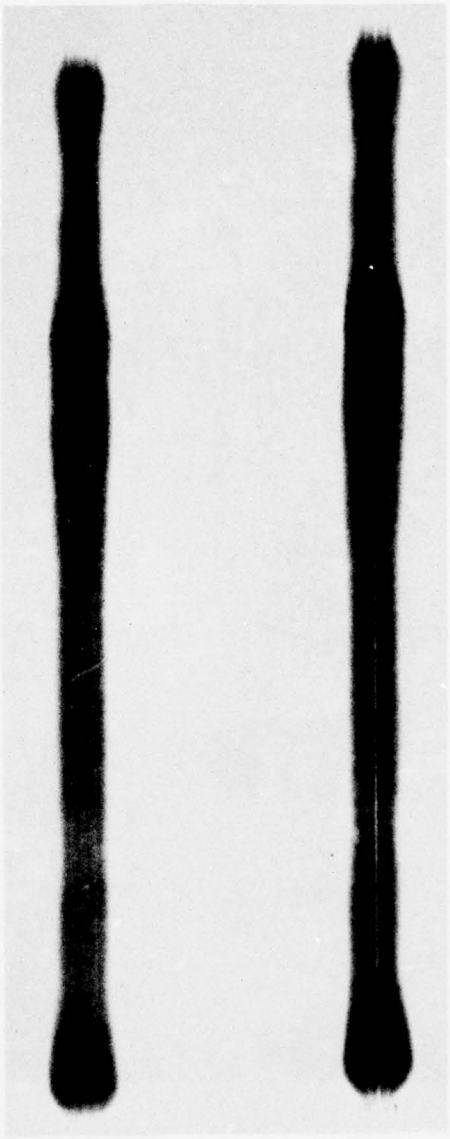

Sample No. 337

H V

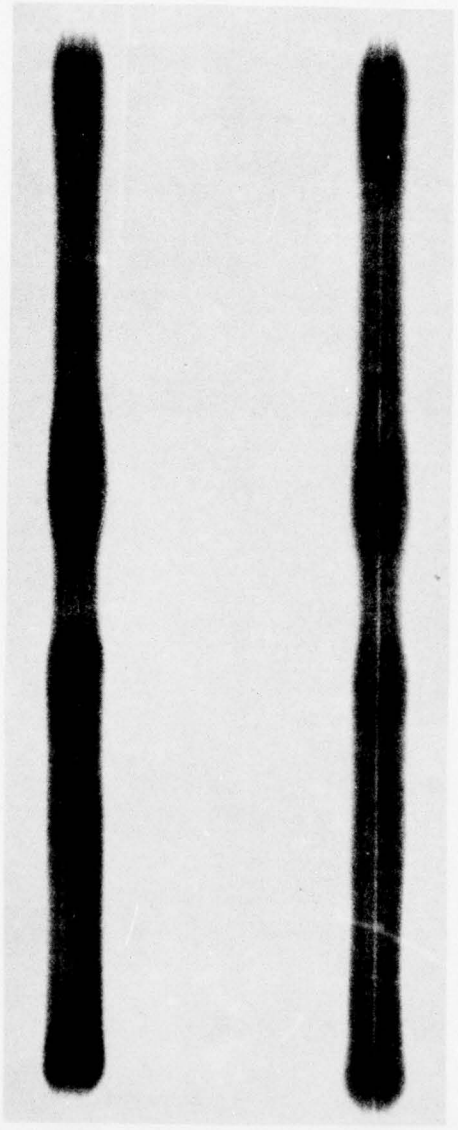

Sample No. 338

DISTRIBUTION LIST

The Institute for Defense Analysis
Science and Technology Division
ATTN: Dr. Alvin D. Schnitzler
400 Army-Navy Drive
Arlington, VA 22202

Commander (2)
US Army Electronics Command
ATTN: DRSEL-PP-I-PI-1
(Mr. W. Peltz)
Fort Monmouth, NJ 07703

Dr. Joseph E. Rowe
Vice Provost and Dean
School of Engineering
Case Western Reserve University
312 Glennan Bldg.
Cleveland, OH 44106

Director, Applied Physics Laboratory
Sperry Research Center
ATTN: Dr. Richard Damon
Sudbury, MA 01776

Dr. Daniel G. Dow, Chairman
Dept. of Electrical Engineering
University of Washington
Seattle, Washington 98195

Commanding General
US Army Electronics Command
ATTN: DRSEL-TL-BM
(Mr. N.M. Wilson)
Fort Monmouth, NJ 07703

Commander
Harry Diamond Labs.
ATTN: AMXDO-RAA
(Mr.H.W.A. Gerlach)
2800 Powder Mill Road
Adelphi, MD 207833

Naval Electronics Laboratory Ctr
ATTN: Mr. E.D. Maynard, Jr.
Code 220
271 Catalina Blvd.
San Diego, CA 92152

Commander, RADC
Surveillance Technology Branch
ATTN: Mr. H. Chiosa, OCTE
Griffiss AFB, NY 13441

Director, National Security Agency
ATTN: Mr. A.T.Andrews, Jr. R335
Fort George G. Meade, MD 20755

Commander
US Army Production Equipment Agency
ATTN: AMXPE-MT (Mr. C.E. McBurney)
Rock Island, IL 61201

Advisory Group on Electron Devices (2)
ATTN: Working Group on Special
Devices
201 Varick Street
New York, NY 10014

Raytheon Company
Microwave and Power Tube Division
ATTN: L.L. Clampitt
190 Willow Street
Waltham, MA 02154

Dr. Turner E. Hasty, Director
Semiconductor, Research and Engr. Labs.
Texas Instruments, Inc.
PO Box 5013, M.S. 72
Dallas, TX 75222

Microwave Associates
ATTN: Dr. Joseph A. Saloom
Burlington, MA 01803

Commanding General
US Army Electronics Command
ATTN: DRSEL-TL-IM
(Mr. V.G.Gelnovatch)
Fort Monmouth, NJ 07703

US Army Ballistic Research Labs.
ATTN: Mr. D.G. Bauerle, AMXBR-CA
Aberdeen Proving Group, MD 21005

Director, US Army Ballistic Missile
Defense Advanced Technology Ctr.
ATTN: ATC-R, Dr. Bob L. Smith
P.O. Box 1500
Huntsville, AL 35807

Department of the Navy
US Naval Research Lab
ATTN: Mr. L. Whicker, Code 5250
Washington, DC 20390

Commander, AFAL
ATTN: AFAL/TE, Mr. J. Edwards
Wright-Patterson AFB, OH 45433

Lincoln Lab., MIT
ATTN: Dr. G.L. Guernsey
PO Box 73
Lexington, MA 02173

DISTRIBUTION LIST (CONTINUED)

AMPEX Corporation
ATTN: Mr. Gil Argentina 3-22
401 Broadway
Redwood City, CA 94063

US Army Missile Command
Directorate for Res. Engr. and
Missile Systems Lab.
ATTN: AMSMI-RLM
(Mr. P. Ormsby)
Redstone Arsenal, AL 35809

Microwave Applications Group
ATTN: Dr. Charles Boyd, Jr.
10021 Canaga Ave.
Chatsworth, CA 91311

US Army Elect Tech and Devices Lab(5)
ATTN: DRSEL-TL-MA
(Mr. Richard Babbitt)
Fort Monmouth, NJ 07703

NASA Headquarters
ATTN: Mr. C. E. Catoe
Code RES
Washington, D.C. 20546

Trans Tech, Inc.
ATTN: Mr. R. West
12 Meem Ave.
Gaithersburg, MD 20760

U.S. Army Missile Command
Director for Res. Engr. and Missile
Systems Lab.
ATTN: AMSMI-REI
(Mr. B. Spalding)
Redstone Arsenal, AL 35809

US Army Combat Surv and Target
Acq. Lab
ATTN: DRSEL-CT-R
Fort Monmouth, NJ 07703

Defense Documentation Center (12)
ATTN: DDC-IRS
Cameron Station (Bldg. 5)
Alexandria, VA 22314

Commander
US Army Electronics Command
ATTN: DRSEL-RD-ET-2
(Mr. Phillip Meltesen)
Fort Monmouth, NJ 07703